

Thermodynamic description of Tc(IV) solubility and carbonate complexation in alkaline NaHCO₃–Na₂CO₃–NaCl systems†

A. Baumann, ^{*a} E. Yalçıntaş,^{a,b} X. Gaona, ^{*a} R. Polly,^a K. Dardenne,^a
T. Prüßmann, ^a J. Rothe,^a M. Altmaier^a and H. Geckeis^a

The solubility of ⁹⁹Tc(IV) was investigated in dilute to concentrated carbonate solutions ($0.01 \text{ M} \leq C_{\text{tot}} \leq 1.0 \text{ M}$, with $C_{\text{tot}} = [\text{HCO}_3^-] + [\text{CO}_3^{2-}]$) under systematic variation of ionic strength ($I = 0.3\text{--}5.0 \text{ M}$ NaHCO₃–Na₂CO₃–NaCl–NaOH) and pH_m ($\log[\text{H}^+] = 8.5\text{--}14.5$). Strongly reducing conditions ($p_e + \text{pH}_m \approx 2$) were set with Sn(II). Carbonate enhances the solubility of Tc(IV) in alkaline conditions by up to 3.5 log₁₀-units compared to carbonate-free systems. Solvent extraction and XANES confirmed that Tc was kept as +IV during the timeframe of the experiments (≤ 650 days). Solid phase characterization performed by XAFS, XRD, SEM-EDS, chemical analysis and TG-DTA confirmed that TcO₂·0.6H₂O(am) controls the solubility of Tc(IV) under the conditions investigated. Slope analysis of the solubility data in combination with solid/aqueous phase characterization and DFT calculations indicate the predominance of the species Tc(OH)₃CO₃[−] at pH_m ≤ 11 and $C_{\text{tot}} \geq 0.01 \text{ M}$, for which thermodynamic and activity models are derived. Solubility data obtained above pH_m ≈ 11 indicates the formation of previously unreported Tc(IV)–carbonate species, possibly Tc(OH)₄CO₃^{2−}, although the likely formation of additional complexes prevents deriving a thermodynamic model valid for this pH_m-region. This work provides the most comprehensive thermodynamic dataset available for the system Tc⁴⁺–Na⁺–Cl[−]–OH[−]–HCO₃[−]–CO₃^{2−}–H₂O(l) valid under a range of conditions relevant for nuclear waste disposal.

1 Introduction

Technetium-99 is a low-energy β-emitter and one of the main fission products of ²³⁵U and ²³⁹Pu in nuclear reactors. Due to its large inventory in spent nuclear fuel, long half-life ($2.1 \times 10^5 \text{ a}$) and redox characteristics, ⁹⁹Tc is a relevant radionuclide in the context of nuclear waste disposal. Tc can be present in different oxidation states with the two most common ones being Tc(VII) under anoxic and oxidizing, and Tc(IV) under reducing conditions. Tc(VII) is known to be highly soluble in aqueous media and forms the mobile TcO₄[−] aqueous species. Under the reducing, alkaline conditions expected in underground repositories for nuclear waste disposal, Tc is found as Tc(IV) which forms the sparingly soluble hydrous oxide TcO₂·xH₂O(am) according to the redox equilibrium $\text{TcO}_4^- + 4\text{H}^+ + 3\text{e}^- \rightleftharpoons \text{TcO}_2 \cdot x\text{H}_2\text{O}(\text{am}) + (2-x)\text{H}_2\text{O}(\text{l})$.

The precise geochemical conditions expected within repositories for nuclear waste are largely defined by the host rock formation, the selected technical barriers (such as cement or bentonite) and the backfill material. Carbonate is a relevant component in the pore water of clay and crystalline systems but is also a major component in cementitious materials. Furthermore, organic waste constituents are considered to degrade to CO₂(g), thus representing a potential anthropogenic source of carbonate.^{1,2} Carbonate forms strong complexes with Lewis acids such as actinides or Tc(IV), and thus can potentially contribute to their mobilization from the repository into the biosphere.

Highly saline solutions ($5 \leq I \leq 15$) may form in the unlikely event of water intrusion in salt-rock repositories, although formation waters with elevated ionic strength are also found in sedimentary bedrocks in the Canadian Shield and Cretaceous argillites in Northern Germany.^{3,4} The chemical behaviour of Tc in these systems can significantly differ from observations made in dilute solutions. Strong ion interaction processes can importantly modify the stability of charged species at elevated ionic strength. The formation of new aquatic species and complexes unknown in dilute systems may also occur in concentrated solutions, as recently reported for An(III/IV/V) and Tc(IV)

^aInstitute for Nuclear Waste Disposal, Karlsruhe Institute of Technology, P.O. Box 3640, 76021 Karlsruhe, Germany. E mail: alexander.baumann@kit.edu, xavier.gaona@kit.edu

^bLos Alamos National Laboratory, Carlsbad, New Mexico 88220, USA

†Electronic supplementary information (ESI) available. See DOI: 10.1039/c8dt00250a

in concentrated CaCl_2 and MgCl_2 brines.^{5–9} As a consequence, the chemical behaviour and mobility of technetium under high ionic strength conditions cannot simply be extrapolated from dilute systems but need to be investigated for particular saline systems.

In spite of its relevance, only a limited number of experimental studies has been dedicated to assessing the solution chemistry of Tc(IV) in carbonate media. The most relevant studies available on this topic in the literature are summarized in the following.

Eriksen *et al.* studied the solubility of Tc(IV) at $6.2 \leq \text{pH} \leq 8.6$ under constant p_{CO_2} (0.01 to 1.0 atm) and $I < 0.01 \text{ M}$.^{10,11} The authors performed all experiments starting from electro-deposited Tc(IV) in absence of reducing agents, which lead to the co-existence of Tc(IV) and Tc(VII) in solution. Although not clearly stated by the authors, the study was likely performed with short-term experiments, which may not represent thermodynamic equilibrium. The authors observed an increase in solubility of Tc(IV) with increasing p_{CO_2} , which was attributed to the formation of the two aqueous Tc(IV)-hydroxo-carbonato complexes $\text{Tc}(\text{OH})_2\text{CO}_3(\text{aq})$ and $\text{Tc}(\text{OH})_3\text{CO}_3^-$ prevailing below and above $\text{pH} \approx 6$, respectively.

In 1999 the Nuclear Energy Agency (NEA) published its first comprehensive thermochemical review for technetium (TDB) in which experimental studies available for technetium were critically reviewed, resulting in the most authoritative thermodynamic selection currently available for this element.¹² The thermodynamic selection for the Tc(IV)-carbonate system was only based on the solubility study by Eriksen and co-workers.^{10,11} The NEA-TDB update book published in 2003 retained the previous thermodynamic selection by Rard and co-workers.^{12,13}

After the publication of the NEA-TDB update book, Liu *et al.* studied the solubility of Tc(IV) in granitic water with $C_{\text{tot}} \approx 9 \times 10^{-4} \text{ M}$ at $\text{pH} = 8.84$.¹⁴ Additional experiments were performed with the same pore water composition but varying pH ($0.5 \leq \text{pH} \leq 12.5$). It appears evident that degassing of $\text{CO}_2(\text{g})$ may have occurred in acidic and near-neutral pH conditions, and thus that carbonate concentration was significantly decreased in this pH -region. Experiments were performed from oversaturation conditions with *in situ* reduction of Tc(VII) ($[\text{Tc}(\text{VII})]_0 = 3 \times 10^{-6} \text{ M}$) using SnCl_2 . Samples were equilibrated for 3 to 7 months. The authors reported that Tc(IV) solubility remained unaffected by this carbonate concentration. A small increase in solubility was observed after increasing the carbonate concentration to $C_{\text{tot}} = 0.1 \text{ M}$, although the authors attributed this observation to the increase in pH caused by the addition of Na_2CO_3 .

Alliot and co-workers performed a potentiometric study on the speciation of Tc(IV) in bicarbonate media at $7 \leq \text{pH} \leq 10$ and $0.01 \text{ M} \leq C_{\text{tot}} \leq 1.0 \text{ M}$.¹⁵ Concentrations of Tc(III), Tc(IV) and Tc(VII) were determined by UV-Vis measurements. Experiments were performed with $10^{-6} \text{ M} \leq [\text{Tc}(\text{VII})] \leq 10^{-4} \text{ M}$ and $10^{-6} \text{ M} \leq [\text{Tc}(\text{IV})] \leq 10^{-4} \text{ M}$. Note that some of these systems were clearly oversaturated with respect to $\text{TcO}_2 \cdot x\text{H}_2\text{O}(\text{am})$, although the authors did not report the formation of any

solid phase. Chemical and thermodynamic models reported by the authors for the Tc(IV)-carbonate system are in good agreement with the current NEA-TDB selection. Based on their observations in solutions containing $0.3 \text{ M} \leq C_{\text{tot}} \leq 0.7 \text{ M}$, Alliot *et al.* also reported the ion interaction coefficient $\epsilon(\text{Tc}(\text{OH})_3\text{CO}_3^-, \text{Na}^+) = -(0.20 \pm 0.15) \text{ kg mol}^{-1}$.

Previous experimental studies avoided the discussion on the structure of the Tc(IV)-carbonate complexes forming in solution. This is expectedly due to the low concentrations of Tc(IV)(aq) in equilibrium with $\text{TcO}_2 \cdot x\text{H}_2\text{O}(\text{am})$ (even in the presence of carbonate), which hinder the use of spectroscopic techniques to elucidate the structure of these complexes. The nomenclature originally proposed by Eriksen and co-workers (*e.g.* $\text{Tc}(\text{OH})_x\text{CO}_3^{4-2-x}$) has been systematically used in subsequent studies (also in the NEA-TDB reviews), but has no sound scientific basis. Experimental observations can be hence equally well described with complexes of the type $\text{TcO}(\text{OH})_y\text{CO}_3^{y-}$, which include the moiety TcO^{2+} . In this context, density functional theory (DFT) calculations can be used to gain relevant insight on the structure and stability of aqueous complexes for systems that cannot be probed spectroscopically. For Tc, this approach was successfully applied in our previous work focusing on the formation of ternary Ca/Mg-Tc(IV)-OH species.^{9,16} This opens the door for the application of DFT to other Tc(IV) systems of relevance, where the formation of sparingly soluble $\text{TcO}_2 \cdot x\text{H}_2\text{O}(\text{am})$ prevents the spectroscopic characterization of the aqueous species.

Despite the relevance of carbonate in the context of nuclear waste disposal, none of the previous investigations performed a systematic Tc(IV) solubility study under a broad range of carbonate concentrations and dilute to concentrated saline solutions. Most of the available studies were restricted to $\text{pH} < 10$, leaving aside the hyperalkaline pH -region which may be buffered in a repository by the different stages of cement degradation ($10 < \text{pH} < 13.3$). Such systems are addressed in the present work, covering dilute to concentrated NaHCO_3 - Na_2CO_3 - NaCl - NaOH solutions, with the final aim of deriving complete chemical, thermodynamic and activity models. This experimental work further benefits from input by DFT calculations, which provide information on the structure of the ternary Tc(IV)-OH- CO_3 complexes forming in the aqueous phase.

2 Experimental

2.1 Chemicals

NaCl (p.a.), NaHCO_3 (p.a.), $\text{Na}_2\text{CO}_3 \cdot 10\text{H}_2\text{O}$ (p.a.), CHCl_3 (p.a.), NaOH (Titrisol®) and HCl (Titrisol®) were purchased from Merck. Tetraphenylphosphonium chloride (TPPC, $\text{C}_{24}\text{H}_{20}\text{ClP}$, 98%) and SnCl_2 (98%) were purchased from Sigma-Aldrich. Ethanol (99%) was purchased from VWR Chemicals. PerkinElmer Ultima Gold™ XR was used as liquid scintillation counting (LSC) cocktail.

A purified and radiochemically well-characterized ^{99}Tc stock solution (1.3 M NaTcO_4) was used for the electro-

chemical preparation of an acidic Tc(IV) stock solution. The resulting Tc(IV) stock solution was subsequently precipitated as $\text{TcO}_2 \cdot 0.6\text{H}_2\text{O}(\text{am})$ under reducing, alkaline conditions ($\text{Na}_2\text{S}_2\text{O}_4$, $\text{pH}_m = 12.5$) and aged for two months.

All sample preparation and handling was performed in an Ar-glovebox at $T = (22 \pm 2)^\circ\text{C}$. All solutions were prepared with ultrapure water purified with a Millipore Milli-Q Advantage A10 (18.2 M Ω cm at 25 $^\circ\text{C}$, 4 ppb TOC) with Millipore Millipak® 40 0.22 μm , purged with Ar for 1 hour before use to remove traces of oxygen and $\text{CO}_2(\text{g})$.

2.2 pH_m and E_h measurements

The determination of the proton concentration ($\text{pH}_m = -\log[\text{H}^+]$, with $[\text{H}^+]$ in molal units) was performed using combination pH electrodes (type ROSS, Orion) calibrated against standard pH buffers ($2 \leq \text{pH} \leq 12$, Merck). In salt solutions of ionic strength $I_m \geq 0.1 \text{ mol kg}^{-1}$, the measured pH value (pH_{exp}) is an operational apparent value related to the molal proton concentration $[\text{H}^+]$ by $\text{pH}_m = \text{pH}_{\text{exp}} + A_m$ (or conversely A_c in molar units),^{17,18} where A_m (A_c) is an empirical correction factor. For a given background electrolyte concentration, the empirical correction factor A_m entails both the liquid junction potential of the electrode and the activity coefficient of H^+ . A_m factors for the respective NaCl solutions at each ionic strength are used as reported by Altmaier *et al.* (2003),¹⁹ assuming a negligible contribution of carbonate. For those samples with $[\text{OH}^-] < 0.01 \text{ M}$, $[\text{CO}_3^{2-}]$ was calculated from pH_m and $C_{\text{tot}} = [\text{HCO}_3^-] + [\text{CO}_3^{2-}]$ by using the auxiliary data provided in the NEA-TDB for the dissociation constants of carbonic acid (corrected to $T = 22^\circ\text{C}$), water activities and SIT coefficients of $\varepsilon(\text{H}^+, \text{Cl}^-) = (0.12 \pm 0.01)$, $\varepsilon(\text{Na}^+, \text{OH}^-) = (0.04 \pm 0.01)$, $\varepsilon(\text{Na}^+, \text{HCO}_3^-) = (0.00 \pm 0.02)$, and $\varepsilon(\text{Na}^+, \text{CO}_3^{2-}) = -(0.08 \pm 0.03) \text{ kg mol}^{-1}$.¹³ For those samples with $[\text{OH}^-] \geq 0.01 \text{ M}$, $[\text{H}^+]$ and activity of water were calculated using thermodynamic data and Pitzer activity coefficients selected in the THEREDA database.^{20,21}

Measurements of the redox potential were performed with Pt combination electrodes with Ag/AgCl reference system (Metrohm) and converted to E_h versus the standard hydrogen electrode by correction for the potential of the Ag/AgCl reference electrode (+208 mV for 3 M KCl at $T = 22^\circ\text{C}$). All samples were measured for 15–30 minutes while agitating continuously. The apparent electron activity ($\text{pe} = -\log a_e$) was calculated from $\text{pe} = 16.9E_h$ [V], according to the equation $E_h = \frac{RT \ln 10}{F} \log a_e$. The performance of the redox electrode was tested with a standard redox buffer solution (+220 mV vs. Ag/AgCl, Schott) and provided readings within $\pm 10 \text{ mV}$ of the certified value.

2.3 Determination of Tc total concentration and redox speciation in solution

Liquid scintillation counting (LSC) was used to quantify the total concentration of Tc in the aqueous phase. For each sample, 500 μl of supernatant were separated and centrifuged in 10 kD filters (2–3 nm cut-off, Nanosep® and Mikrosep® Pall Life Sciences) at 4020g for 7 minutes to separate colloids

or suspended solid phase particles. 400 μl of this solution were then pipetted into 600 μl of 1.0 M HCl. 600 μl of the acidified solution were added to 10 ml of LSC cocktail (PerkinElmer Ultima Gold™ XR) in a screw-cap (PP, 20 ml, Zinsser Analytic) and measured by a LKB Wallac 1220 Quantulus Liquid Scintillation Counter for 30 minutes each. The background count rate was determined by repeated measurements of inactive blanks, and the resulting detection limit (3 times the standard deviation of the blank) was calculated as $7.9 \times 10^{-10} \text{ M}$.

Liquid–liquid extraction (LLE) was used for the quantification of Tc(IV) in the aqueous phase. 500 μl of the supernatant of selected solubility samples were centrifuged in 10 kD filters at 4020g. 400 μl of the filtered solution were acidified with 4.0 M HCl and pipetted into 400 μl of a solution of 50 mM TPPC in chloroform and shaken for 60 seconds.²² After subsequent separation of the aqueous and organic phases by centrifugation, the technetium concentration in the aqueous phase was determined by LSC and attributed to the presence of Tc(IV).

2.4 Solubility experiments in carbonate solutions

Three independent series of undersaturation solubility experiments were prepared with $\text{TcO}_2 \cdot x\text{H}_2\text{O}(\text{am})$ in the presence of carbonate:

- $C_{\text{tot}} = [\text{HCO}_3^-] + [\text{CO}_3^{2-}] = 0.01, 0.05, 0.1$ and 0.5 M , with constant $I = 5.0 \text{ M}$ (NaHCO_3 – Na_2CO_3 – NaCl) at $8.5 \leq \text{pH}_m \leq 12$;
- Constant $C_{\text{tot}} = [\text{HCO}_3^-] + [\text{CO}_3^{2-}] = 0.05$ and 0.1 M , with $I = 0.3, 0.5, 1.0, 3.0$ and 5.0 M (NaHCO_3 – Na_2CO_3 – NaCl) at $8.5 \leq \text{pH}_m \leq 12$;
- $C_{\text{tot}} = [\text{CO}_3^{2-}]_{\text{tot}} = 0.1, 0.5$ and 1.0 M , with $[\text{OH}^-] = 0.01$ to 0.6 M (Na_2CO_3 – NaOH mixtures, absence of NaCl).

This experimental scheme resulted in a total of 62 independent samples. To ensure the stabilization of Tc in its tetravalent state and to avoid oxidation, 2 mM SnCl_2 were added as reductant to all samples.^{23,24} pH_m and E_h values of prepared background electrolytes were measured after 2 weeks to ensure that stable pH_m values and the necessary reducing conditions for Tc(IV) were reached. After confirmation that all solutions were properly pre-equilibrated, 2–3 mg of Tc(IV) solid were washed three times with 1 ml of the matrix solution and then added to 20 ml of matrix solution to form the final samples in 50 ml screw cap centrifuge vials (Nalgene™, Thermo Scientific). pH_m , E_h and Tc concentrations in the solubility samples were measured at regular time intervals for up to 636 days. A limited number of samples with $\text{pH}_m \leq 9$ showed a slight increase of pH_m (≤ 0.2) in the course of the measurements, which was attributed to the formation of $\text{CO}_2(\text{aq})$ and consequent degassing of $\text{CO}_2(\text{g})$. The loss of carbonate due to the degassing of $\text{CO}_2(\text{g})$ was quantified as $< 10\%$ of C_{tot} , considering the values of pH_m , ΔpH_m and initial C_{tot} .

2.5 Solid phase characterization

After attaining equilibrium conditions, the solid phase of selected solubility samples was characterized using X-ray diffraction (XRD), quantitative chemical analysis, scanning electron microscope-energy dispersive spectrometry (SEM-EDS) and

thermogravimetric analysis (TG-DTA). Approximately 1 mg of solid containing Tc(IV) was washed three times with ethanol inside the Ar-glovebox to remove the salt-containing background electrolyte solution. The washed solid was suspended in $\approx 10 \mu\text{l}$ of ethanol, transferred to a capped silicon single crystal sample holder (Dome, Bruker), dried under an Ar-atmosphere for a few minutes before sealing of the sample holder, and transferred outside the glovebox for the collection of the XRD diffractogram. Measurements were performed on a Bruker AXS D8 Advance X-ray powder diffractometer (Cu-K α radiation) at measurement angles $2\theta = 5\text{--}100^\circ$ with incremental steps of 0.02° and a measurement time of 9 seconds per increment. After the XRD measurement, the solid phase was dissolved in 1 ml of 2% HNO $_3$ and analysed by LSC and ICP-OES (inductively coupled plasma-optical emission spectroscopy) to determine the concentration of technetium and sodium, respectively. ICP-OES measurements were performed with a PerkinElmer OPTIMA 2000TM. A second fraction of the washed solid was characterized by SEM-EDS (FEI Quanta 650 FEG equipped with a Noran EDS unit) for qualitatively assessing the morphology and particle size of the Tc(IV) solid phases.

Thermogravimetric analysis (TG-DTA) was performed to determine the number of hydration waters in the original TcO $_2 \cdot x\text{H}_2\text{O}(\text{am})$ solid phase. TG-DTA measurements were conducted using a Netzsch STA 449C thermo-microbalance. 8.7 mg of Tc(IV) solid was washed 3 times with ethanol. The salt-free solid phase was left to dry for 3 days under Ar-atmosphere. The measurements were then performed, also under Ar-atmosphere, by increasing the temperature with steps of 5°C per minute up to a final temperature of 200°C .

2.6 XANES and EXAFS measurements

EXAFS/XANES spectra were recorded at the ACT-Beamline for Actinide Research (2.5 T superconducting wiggler source)²⁵ at the 2.5 GeV KIT-synchrotron radiation source,²⁶ KIT Campus North.

Both solid and aqueous phases were characterized by XAFS to evaluate the redox state of Tc and assess its coordination environment. Three reference samples were measured by XANES: (i) a 1×10^{-3} M TcO $_4^-$ solution at $\text{pH}_m \approx 1$, (ii) the original TcO $_2 \cdot 0.6\text{H}_2\text{O}(\text{am})$ material before contacting carbonate solutions and (iii) the corresponding Tc(IV) aqueous supernatant at $\text{pH}_m \approx 12.5$ (absence of carbonate, $[\text{Tc}] \approx 3.8 \times 10^{-5}$ M). Two aqueous and one solid samples were selected for XANES measurements: (i) the supernatant solution of the sample equilibrated in 1.0 M Na $_2\text{CO}_3$ with 0.6 M NaOH ($[\text{Tc}] \approx 1.2 \times 10^{-5}$ M), (ii) the supernatant solution of the sample equilibrated in 0.1 M Na $_2\text{CO}_3$ ($I = 5.0$ M) at $\text{pH}_m = 9.5$ ($[\text{Tc}] \approx 1.5 \times 10^{-6}$ M) and (iii) the solid phase of the sample equilibrated in 1.0 M Na $_2\text{CO}_3$ with 0.1 M NaOH ($[\text{Tc}] \approx 1.0 \times 10^{-5}$ M). Two Tc solid samples equilibrated in carbonate systems were selected for EXAFS measurements: (i) the solid phase equilibrated in 1.0 M Na $_2\text{CO}_3$ with 0.6 M NaOH and (ii) solid phase equilibrated in 0.1 M Na $_2\text{CO}_3$ with $I = 5.0$ M at $\text{pH}_m = 9.5$.

In all cases, approximately 300 μL of the suspension were transferred to a 400 μL polyethylene vial under Ar-atmosphere and centrifuged at 4020g for 10 minutes to obtain a com-

packed solid phase at the bottom of the vial. The vials were mounted in a gas-tight cell with windows of Kapton® film (polyimide) inside an Ar-glovebox and transported to the ACT-Beamline, where it was kept under continuous flow of Ar during the course of the measurements.

A pair of Si(311) crystals is used in the double crystal monochromator (DCM, FMB Oxford, Oxford, United Kingdom). The monochromatic radiation delivered by the DCM is focused by a Rh-coated toroidal mirror into a spot-size below 1 mm diameter at the sample position. The intensity of the beam is optimized at 21.5 keV. The intensity of the incoming beam (I $_0$) is monitored using an Ar-filled ionization chamber at ambient pressure. A five pixel LEGe solid state detector (Canberra, Olen, Belgium) is used for collecting Tc K α fluorescence radiation. The fluorescence signal emitted by the sample is analyzed and filtered by a digital X-ray pulse processing system (XMAP DXP module, XIA LLC, Hayward (CA), USA). Tc K-edge XAFS spectra of liquid samples are recorded in fluorescence detection mode by registering the Tc K $\alpha_{1,2}$ fluorescence yield (18.367 keV (K α_1) and 18.251 keV (K α_2)) as a function of the incident photon energy. For solid samples XAFS spectra are recorded simultaneously in fluorescence and transmission mode. The Tc K-edge spectra ($E(\text{Tc}^0 1s) = 21.044$ keV) are calibrated against the first derivative X-ray absorption near edge structure (XANES) spectrum of a molybdenum metal foil (energy of first inflection point set to $E(\text{Mo}^0 1s) = 20.000$ keV) recorded simultaneously.

XAFS data analysis is based on standard procedures, normalizing energy calibrated XANES spectra to their edge-jump and fitting a model to EXAFS $\chi(k)$ data as implemented in the Demeter suit of programs version 0.9.26.²⁷

The k -range used in the modelling was $[3.1\text{--}10.85 \text{ \AA}^{-1}]$. Fits were performed in the R -space $[1.1\text{--}2.8 \text{ \AA}]$ using simultaneously the k -, k^2 -weighted data. The overall intensity factor (S^0) is set to 0.90 during the fit. The structure of TcO $_2$ (ICSD 173151) was used as model to fit the data.

2.7 Density functional theory (DFT) calculations

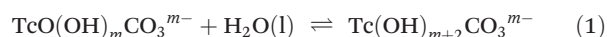
The relative stability of the species Tc(OH) $_m\text{CO}_3^{m-}$ and Tc(OH) $_{m+2}\text{CO}_3^{m-}$ (with $m = 1\text{--}2$) was investigated using DFT calculations. TcO $^{2+}$ is the moiety at the core of the species Tc(OH) $_m\text{CO}_3^{m-}$. The ground state of this moiety was already determined and characterized by CASSCF calculations in our previous work.¹⁶ Two low lying states were found for these species: $^2\Delta$ with an equilibrium distance of 155 pm, and $^4\Pi$ with an equilibrium distance of 165 pm. The state $^2\Delta$ has the lowest energy at 155 pm, but $^4\Pi$ becomes more stable already at 165 pm. This is important since the coordination of OH-ligands to the TcO $^{2+}$ moiety increases the distance r_{TcO} , and consequently the $^4\Pi$ state becomes the ground state of the Tc(OH) $_m\text{CO}_3^{m-}$ species.

The ground states of the species Tc(OH) $_{m+2}\text{CO}_3^{m-}$ were determined in the present work using RASSCF and CASSCF multi reference methods as implemented in MOLCAS.²⁸ For the RASSCF and CASSCF calculations the ANO-RCC-VDZ basis sets were used.^{29–31} The RASSCF calculations served to determine a suitable active space for the CASSCF calculations. For

this all the 2p orbitals of the oxygen atoms and the 4s and 4p orbitals of technetium were selected to form the RAS1 space. The RAS2 space consists of the five 4d orbitals of technetium and the RAS3 space is formed by the 5s and 5p orbitals of technetium. These RASSCF calculations give a clear picture about the orbitals that should be kept inactive or active in the final CASSCF calculations on the $\text{Tc}(\text{OH})_{m+2}\text{CO}_3^{m-}$ species. Orbitals with an occupation $0.02 < n < 1.98$ in the RASSCF calculations are considered active and in all other cases they are set either inactive or virtual.

The equilibrium structures of the $\text{Tc}(\text{OH})_{m+2}\text{CO}_3^{m-}$ species were determined with DFT(BP86) employing the TZVPP basis set.³² TURBOMOLE was used for the DFT calculations.^{33–39} This is in this case justified, since the structures are not that sensitive to whether the DFT or the RASSCF/CASSCF method is employed and DFT structures give a very good estimate for the structures obtained with multi reference methods. The equilibrium structures determined with DFT(BP86/TZVPP) were used afterwards to carry out the multi reference RASSCF/CASSCF calculations.

In a second step the reaction energies (ΔE) of reaction (1) were calculated with DFT(BP86/TZVPP). The reaction energies calculated from the electronic energies of the optimized systems were considered as a reasonably good approximation for the Gibbs free energy ($\Delta G \sim \Delta E$).



These theoretical calculations provide key insights on the discussion of the stability of $\text{TcO}(\text{OH})_m\text{CO}_3^{m-}$ vs. $\text{Tc}(\text{OH})_{m+2}\text{CO}_3^{m-}$ complexes. Calculations were performed (i) for the naked species in the gas phase, (ii) including solvation effects by means of the COSMO method and (iii) considering explicitly a solvation shell of 100 water molecules. The structure of this water cluster consisting of 100 molecules was used from the work of Lenz *et al.* (2009).^{40,41}

3 Results and discussion

3.1 Solubility of Tc(IV) in the presence of carbonate

3.1.1 NaHCO_3 – Na_2CO_3 – NaCl systems at $8.5 \leq \text{pH}_m \leq 11.5$. Very reducing conditions ($\text{pe} + \text{pH}_m \approx 2$ –4, see Table SI 1 in the ESI†) were measured in all solubility samples, supporting the predominance of Tc(IV) in the investigated carbonate systems. Fig. 1a, b and c show the Tc solubility data obtained in NaHCO_3 – Na_2CO_3 – NaCl systems with $8.5 \leq \text{pH}_m \leq 11.5$. For better readability, the figures include only data in equilibrium conditions (constant pH_m and [Tc] readings). Note that a very long contact time ($t \geq 275$ days) was required to attain equilibrium in most of the investigated solubility samples. The results are compared to model calculations using thermodynamic data reported in Yalcintas *et al.* (2016)⁹ for solubility and hydrolysis, in combination with thermodynamic data and SIT interaction coefficients for Tc(IV)–carbonate aqueous species ($\text{Tc}(\text{OH})_2\text{CO}_3(\text{aq})$ and $\text{Tc}(\text{OH})_3\text{CO}_3^-$) as selected in the NEA–TDB and reported in Alliot *et al.* (2009), respectively.^{12,15}

Fig. 1a, b and c show a very important impact of carbonate on the solubility of Tc(IV) (up to 3.5 \log_{10} -units) for all investigated systems. Even at the lowest carbonate concentration investigated ($C_{\text{tot}} = 0.01$ M, Fig. 1a), the solubility increases by 1–2 orders of magnitude (depending upon pH_m) compared to carbonate-free systems. For the same C_{tot} , the variation of ionic strength has a relatively minor impact on the solubility (see Fig. 1b and c), thus pointing towards the predominance of low-charged Tc species in the aqueous phase. This is consistent with the predominance of $\text{Tc}(\text{OH})_3\text{CO}_3^-$, predicted using the chemical and thermodynamic models selected in the NEA–TDB.¹² Note that for analogous NaHCO_3 – Na_2CO_3 – NaCl systems and pH_m conditions, Altmaier and co-workers reported a very strong impact of ionic strength on the solubility of Th(IV).⁴² The thermodynamic and activity models derived by the latter authors highlighted the predominant role of the

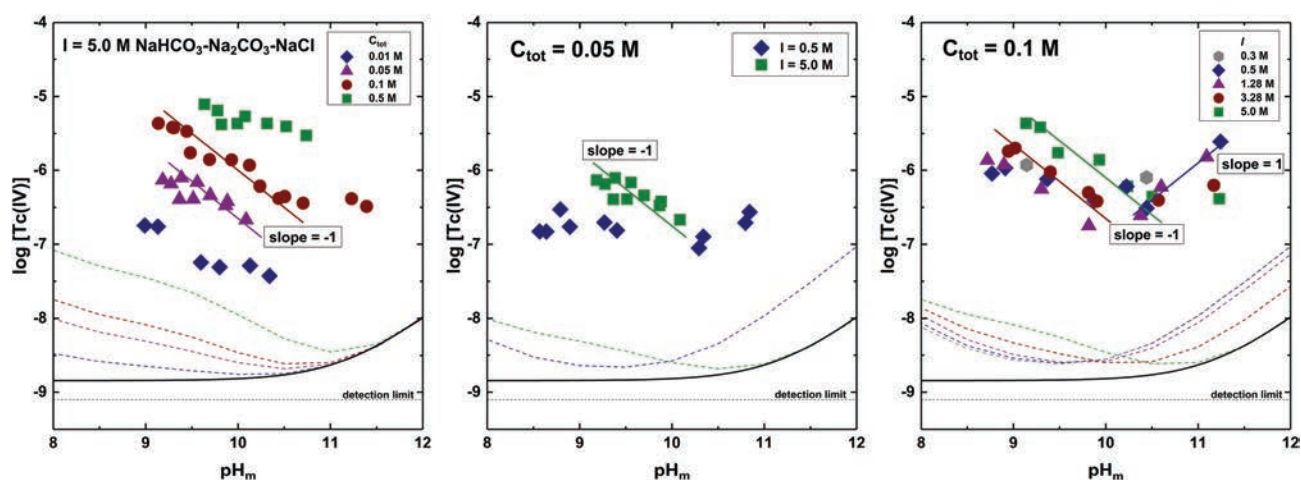


Fig. 1 Experimental solubility data of Tc(IV) in NaHCO_3 – Na_2CO_3 – NaCl systems at $8.5 \leq \text{pH}_m \leq 11.5$. Dashed lines correspond to Tc(IV) solubility in the presence of carbonate calculated using thermodynamic and SIT activity models reported in the NEA–TDB, Alliot *et al.* (2009) and Yalcintas *et al.* (2016).^{9,13,15} Black solid line provides the reference Tc(IV) solubility in 5.0 M NaCl and absence of carbonate, as calculated with thermodynamic and SIT activity models reported in Yalcintas *et al.* (2016).⁹ Solid coloured lines are eye guiding and do not represent any calculated model.

highly charged $\text{ThOH}(\text{CO}_3)_4^{5-}$ species, which justified the strong impact of ionic strength on solubility. The different chemical behaviour of Tc(IV) and Th(IV) can be largely attributed to differences in the size of the corresponding cations ($r_{\text{Tc}^{4+}} = 0.645 \text{ \AA}$ (for CN = 6)⁴³ and $r_{\text{Th}^{4+}} = 1.09 \text{ \AA}$ (for CN = 9)).⁴⁴

Slope analysis ($\log[\text{Tc}]$ vs. pH_m) in Fig. 1a, b and c allows the identification of three different regions in the solubility of Tc in the presence of carbonate:

- region I, $\text{pH}_m < 9$: the solubility of Tc is almost pH_m -independent, with slope ≈ 0 in the less alkaline conditions. This observation implies that no H^+ are being exchanged in the equilibrium reaction controlling the solubility of Tc in this pH_m -region.

- region II, $9-9.5 \leq \text{pH}_m \leq 10-10.5$: decrease of the solubility with slope ≈ -1 , indicating that 1 H^+ is consumed in the equilibrium reaction controlling the solubility of Tc.

- region III, $\text{pH}_m > 10-10.5$: increase in solubility with increasing pH_m . The number of experimental points in this region is too scarce as to provide a defined slope, but the solubility behaviour indicates a release of H^+ in the equilibrium reaction controlling the solubility of Tc.

The trends in Tc solubility observed in regions I and II are similar to those calculated with the chemical and thermodynamic models selected in the NEA-TDB for the Tc(IV)-carbonate system, which predicts the predominance of $\text{Tc}(\text{OH})_3\text{CO}_3^-$ in both regions. Indeed, the change in the slope of the solubility data with increasing pH_m (slope ≈ 0 in region I \rightarrow slope -1 in region II) is related to the change in the speciation of carbonate, from HCO_3^- to CO_3^{2-} ($\text{p}K'_{a2}$ ($I = 0.5 \text{ M NaCl}$, $T = 22 \text{ }^\circ\text{C}$) = 9.67; $\text{p}K'_{a2}$ ($I = 5.0 \text{ M NaCl}$, $T = 22 \text{ }^\circ\text{C}$) = 9.52). On the other hand, the current NEA-TDB model largely underestimates the measured concentrations of Tc. A detailed discussion on this disagreement is provided in section 3.6.1.

The trend in solubility observed in region III is not reproduced by the thermodynamic model selected in the NEA-TDB, and possibly hints towards the formation of additional, previously unreported, Tc(IV)-carbonate species. The positive slope inherently hints towards an increased number of OH-groups in the coordination sphere of Tc, and thus complexes of the type $\text{Tc}(\text{OH})_{3+n}\text{CO}_3^{-(n+1)}$ with $n \geq 1$ should possibly be expected.

Solubility data in Fig. 1a can also be used to extract additional information on the stoichiometry Tc:CO₃ of the complex(es) forming in solution. Hence, Fig. 2 shows $\log[\text{Tc}]$ as a function of $\log C_{\text{tot}}$, as determined in the solubility series with $I = \text{constant} = 5.0 \text{ M NaHCO}_3\text{-Na}_2\text{CO}_3\text{-NaCl}$ at $\text{pH}_m \approx 9.8$ and 10.1. For both values of pH_m evaluated, the solubility tends to follow a slope ($\log[\text{Tc}]$ vs. $\log C_{\text{tot}}$) of +1, thus indicating that the complex forming in these conditions has a ratio Tc:CO₃ of 1:1.

3.1.2 Na₂CO₃-NaOH systems at $[\text{OH}^-] \geq 0.01 \text{ M}$. Fig. 3 shows Tc solubility data in solutions with $C_{\text{tot}} = [\text{CO}_3^{2-}] = 0.1 \text{ M}$, 0.5 M and 1.0 M at $0.01 \text{ M} \leq [\text{OH}^-] \leq 0.6 \text{ M}$. Experimental data are compared with model calculations using thermodynamic data available for Tc(IV) solubility, hydrolysis and carbonate complexation.^{9,12,15} Note however that the currently

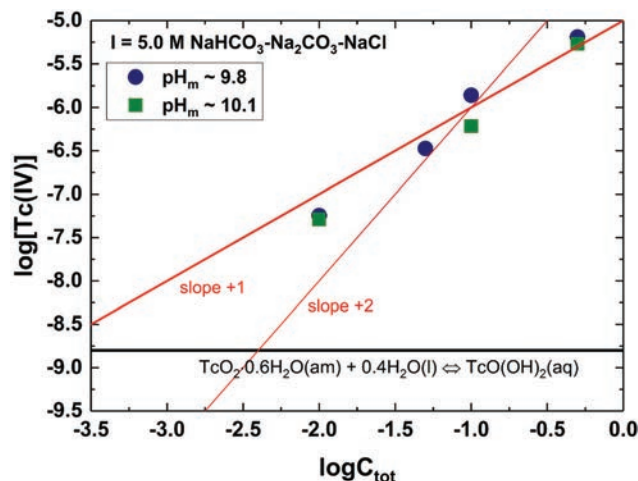


Fig. 2 Experimental solubility data of Tc(IV) in 5.0 M NaHCO₃-Na₂CO₃-NaCl systems with $0.01 \text{ M} \leq C_{\text{tot}} \leq 0.5 \text{ M}$ and $\text{pH}_m \approx 9.8$ and 10.1. Black solid line provides the reference Tc(IV) solubility in carbonate free 5.0 M NaCl, as calculated with thermodynamic and SIT activity models reported in Yalcintas *et al.* (2016).⁹

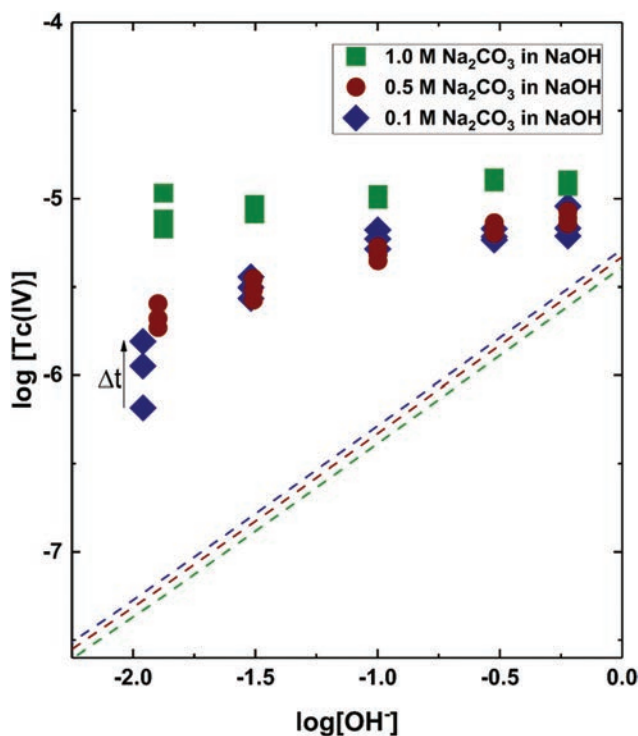


Fig. 3 Experimental solubility data of Tc(IV) in Na₂CO₃-NaOH systems with $[\text{OH}^-] \geq 0.01 \text{ M}$ (symbols), and calculated solubility using thermodynamic and SIT activity models reported by Yalcintas *et al.* (2016) (dashed lines). Δt represents increasing equilibration time and equals ≈ 200 days.⁹

defined Tc(IV)-carbonate species, $\text{Tc}(\text{OH})_2\text{CO}_3(\text{aq})$ and $\text{Tc}(\text{OH})_3\text{CO}_3^-$, cannot outcompete hydrolysis in this range of $[\text{OH}^-]$, and thus $\text{TcO}(\text{OH})_3^-$ is the main aqueous species underlying the calculated solubility curve in Fig. 3.

Very slow kinetics are observed in all investigated Na_2CO_3 - NaOH systems, and equilibrium conditions are only attained after >300 days of contact time (see Fig. 4). Such very long equilibration times are unexpected for solubility equilibria, especially when resulting in the increase of Tc concentration in solution with time. The inverse effect (*i.e.* slow decrease of metal concentration in solution) is normally explained by the increase of particle size in the solid phase controlling solubility (Ostwald ripening).⁴⁵ Experimental observations in the present study may hint towards slow redox transformations or formation of polyatomic species in the aqueous phase. The possible contribution of Tc(VII) to the observed increase of solubility is discussed in detail in sections 3.2 and 3.4. Note that the formation of polyatomic species was also argued by Poineau (2004) and Yalcintas *et al.* (2016) to explain the very slow equilibration kinetics in their solubility experiments with Tc(IV) under acidic conditions.^{9,46}

Fig. 3 and 4 show that the solubility of Tc is largely impacted by carbonate (up to 2 orders of magnitude) also under hyperalkaline pH_m conditions, although the effect on the solubility becomes less relevant with increasing pH_m . In 1.0 M Na_2CO_3 systems, the solubility of Tc remains independent of $[\text{OH}^-]$, whereas a slight trend of increasing $[\text{Tc}]$ with increasing $[\text{OH}^-]$ is observed in 0.1 M Na_2CO_3 solutions. Such differences in the slope analysis may reflect changes in the aqueous speciation of Tc occurring with increasing $[\text{CO}_3^{2-}]$. Note however that ionic strength does not remain constant throughout the experimental series with increasing $[\text{OH}^-]$, and thus changes in the activity coefficients along the series may also impact a correct interpretation of the slope. This is especially true for the series with the lowest $[\text{Na}_2\text{CO}_3]$, where ionic strength varies from 0.3 to 0.9 M along the solubility series.

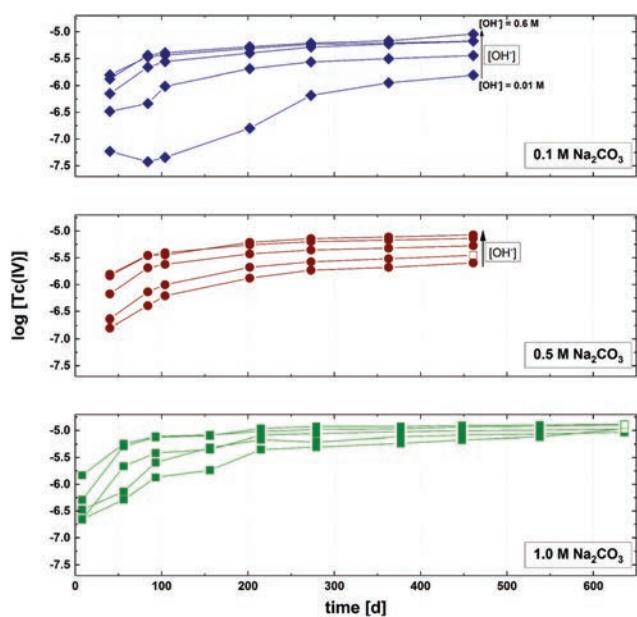


Fig. 4 Experimental solubility data of Tc(IV) as a function of time in Na_2CO_3 - NaOH systems with $[\text{OH}^-] \geq 0.01$ M. Samples selected for XANES measurements are marked as open, square symbols.

Table 1 Fraction of Tc(IV) in the aqueous phase of selected samples with $\text{pH}_m \leq 10$ after liquid-liquid extraction with TPPC

C_{tot} [mol l ⁻¹]	I [mol l ⁻¹]	pH_m^a	Tc(IV)^b [%]
0.01	5.0	9.6	99
0.05	5.0	9.4	94
0.1	5.0	9.5	99
0.5	5.0	9.8	95
0.05	0.5	9.3	93
0.1	0.3	9.1	99
0.1	0.5	9.4	96
0.1	1.28	9.3	97
0.1	3.28	9.4	98

^a ± 0.05 . ^b $\pm 10\%$.

3.2 Tc redox speciation

The results of liquid-liquid extraction are shown in Table 1 as the fraction of Tc(IV) in the supernatant of selected solubility samples. In combination with E_h measurements discussed above and summarized in Table SI 1 in the ESI,[†] liquid-liquid extraction confirms the predominance of Tc(IV) in all the samples evaluated with $\text{pH}_m \leq 10$. Liquid-liquid extraction of samples at hyperalkaline conditions were inconclusive, indicating largely disperse but relevant contributions of Tc(VII) . Replicates collected for selected samples lead also to strongly varying fractions of $\text{Tc(VII)}/\text{Tc(IV)}$. Note however that E_h values confirmed reducing conditions in all samples measured (see Table SI 1[†]) where, from a thermodynamic perspective, the formation of Tc(VII) or other redox states apart from Tc(IV) is not expected. Provided the moderately high $[\text{Tc}]$ in some of the problematic samples (10^{-5} - 10^{-6} M) and the very high sensitivity of the ACT-Beamline for the measurement of Tc, the redox state of Tc in the aqueous phase of selected solubility samples under hyperalkaline pH_m conditions was therefore further investigated by XANES (see section 3.4).

3.3 Solid phase characterization

The very broad XRD patterns observed for the Tc(IV) solid in carbonate samples with $C_{\text{tot}} = 0.1$ M at $I = 0.5$ ($\text{pH}_m = 9.5$) and 5.0 M ($\text{pH}_m = 9.5$), $C_{\text{tot}} = 0.01$ M at $I = 5.0$ M ($\text{pH}_m = 9.8$) and $C_{\text{tot}} = 1.0$ M with $[\text{OH}^-] = 0.6$ M (Fig. 5) are analogous to those previously reported in carbonate-free NaCl solutions and can be attributed to $\text{TcO}_2 \cdot x\text{H}_2\text{O(am)}$.⁹ Sharp features corresponding to NaCl (PDF 05-0628) and Na_2CO_3 (PDF 18-1208) are observed in the solid phases equilibrated at $I = 5.0$ M and at $C_{\text{tot}} = [\text{CO}_3^{2-}] = 1.0$ M, respectively, indicating that the washing step was insufficient to completely remove the NaCl or Na_2CO_3 background electrolytes. The additional peaks visible at $2\theta = 28.6^\circ$ and at $2\theta = 30.3^\circ$ correspond to NaCl and are caused by the instrumental background ($\text{Cu-K}\beta$ radiation of the X-ray source and $\text{W-L}\alpha_1$ radiation produced by the tungsten filament (cathode)).

In agreement with the data obtained by XRD, the SEM images of all selected samples show the predominant presence of amorphous Tc aggregates (see ESI Figure SI 2[†]). Four different solid phases marked in the figure as “A”, “B”, “C” and “D” can be identified. In agreement with XRD patterns

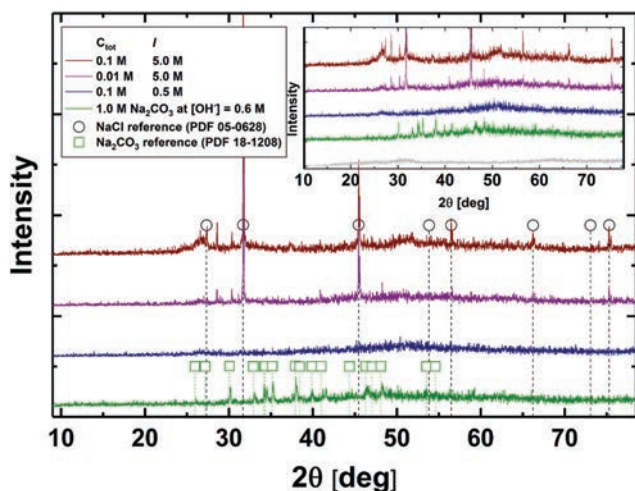


Fig. 5 XRD spectra collected for Tc(IV) solid phases contacted with solutions with $C_{\text{tot}} = 0.1$ M at $I = 0.5$ and 5.0 M, $C_{\text{tot}} = 0.01$ M at $I = 5.0$ M and $C_{\text{tot}} = [\text{CO}_3^{2-}] = 1.0$ M with $[\text{OH}^-] = 0.6$ M. Insert corresponding to a zoom of the amorphous background. XRD spectra reported in Yalcintas *et al.* (2016) for $\text{TcO}_2 \cdot 0.6\text{H}_2\text{O}(\text{am})$ equilibrated in 0.5 M NaCl appended in insert for comparison (grey spectrum).

exhibited by solid phases equilibrated in solutions with $C_{\text{tot}} = 0.1$ M at $I = 5.0$ M and $C_{\text{tot}} = 0.01$ M at $I = 5.0$ M, EDS analysis identifies the crystalline structure “A” as NaCl. In the sample contacted with a solution of $[\text{CO}_3^{2-}] = 1.0$ M and $[\text{OH}^-] = 0.6$ M, the cone-/flower-like structure “B” can be identified as Na_2CO_3 . The needle-like structure “C” corresponds to a tin-containing compound (likely $\text{SnO}(\text{s})$ or $\text{Sn}_6\text{O}_4(\text{OH})_4(\text{s})$)⁴⁷ whereas Tc is the main component of the amorphous aggregates “D”. The particle size of the amorphous Tc aggregates ranges within 35–60 nm. For those samples without NaCl or Na_2CO_3 secondary phases, quantitative chemical analysis (LSC and ICP-OES) confirms the absence of sodium in the Tc solid phase ($\text{Na} : \text{Tc}$ ratio ≤ 0.1).

The number of hydration waters in the original $\text{TcO}_2 \cdot x\text{H}_2\text{O}(\text{am})$ material determined by TG-DTA resulted in $x = (0.5 \pm 0.1)$. This finding agrees well with the value of $x = (0.6 \pm 0.3)$ determined by Yalcintas and co-workers for $\text{TcO}_2 \cdot x\text{H}_2\text{O}(\text{am})$ solid phases equilibrated in NaCl, CaCl_2 and MgCl_2 solutions for a similar time frame.⁹ In accordance with the solid phase characterization summarized above and consistent with our previous Tc(IV) solubility studies,^{9,48} the solid phase controlling the solubility of Tc(IV) in carbonate systems over the entire pH_m -range is defined as $\text{TcO}_2 \cdot 0.6\text{H}_2\text{O}(\text{am})$.

3.4 XANES and EXAFS measurements

A total of 6 samples were measured by XANES and the resulting spectra are shown in Fig. 6 for (i) the original Tc(VII) stock solution used for electrochemical reduction of Tc(IV), (ii) the electrochemically reduced Tc(IV) solid phase ($\text{TcO}_2 \cdot 0.6\text{H}_2\text{O}(\text{am})$), (iii) the corresponding Tc(IV) aqueous supernatant at $\text{pH}_m \approx 12.5$ (absence of carbonate, $[\text{Tc}] \approx 3.8 \times 10^{-5}$ M), (iv) the supernatant solution of the sample equilibrated in $C_{\text{tot}} = 0.1$ M ($I = 5.0$ M) at $\text{pH}_m = 9.5$ ($[\text{Tc}] \approx 1.5 \times 10^{-6}$ M), (v) the

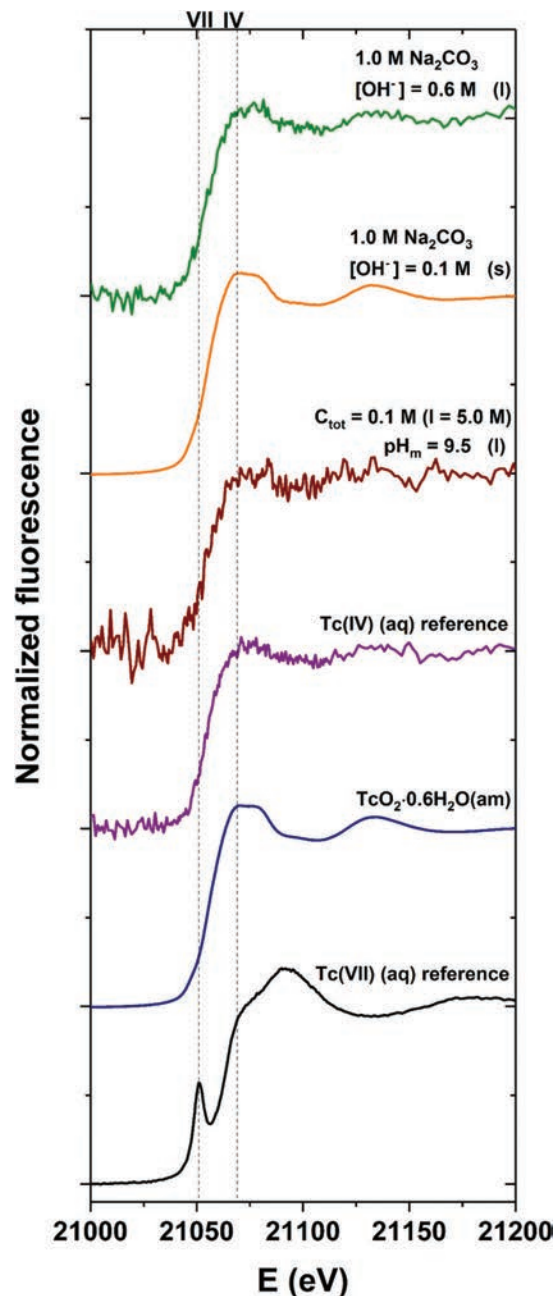


Fig. 6 Tc K edge XANES spectra of Tc(VII) reference, original Tc(IV) solid phase ($\text{TcO}_2 \cdot 0.6\text{H}_2\text{O}(\text{am})$), Tc(IV) liquid reference sample and selected carbonate containing samples.

solid phase of the sample equilibrated in $[\text{CO}_3^{2-}] = 1.0$ M with 0.1 M NaOH ($[\text{Tc}] \approx 1.0 \times 10^{-5}$ M) and (vi) the supernatant solution of the sample equilibrated in $[\text{CO}_3^{2-}] = 1.0$ M with 0.6 M NaOH ($[\text{Tc}] \approx 1.2 \times 10^{-5}$ M).

The shape of the individual XANES spectra and the energy position of the respective inflection points unequivocally prove the sole presence of Tc(IV) above the detection limit of the technique ($<10\%$ in mol-fraction) in all investigated samples. These results are in line with the predominance of Tc(IV) expected in accord with the very reducing (pe + pH_m) values imposed by

Sn(II), and disregard the possible presence of Tc(VII) hinted by liquid-liquid extraction in samples at $\text{pH}_m > 10$. The absence of a pre-peak (transition $1s \rightarrow 4d$ signature) characterising Tc(V) and Tc(VII) allows also to disregard the presence of Tc(V) or Tc(VII) in our samples.^{49–51} The presence of Tc(I) can be ruled out as the edge position will be shifted around 2 eV to lower energy compared to Tc(IV) as reported in Lukens *et al.* which is clearly not the case in our samples.⁵¹ Conclusive XANES reference spectra of Tc(III) are missing so far in the literature. The formation of this redox state of Tc has been reported in highly acidic conditions or in the presence of chelating ligands (EDTA, DMSA *etc.*), and thus can be disregarded in the context of our work.^{52,53}

The k^2 -weighted EXAFS spectra and Fourier Transform (FT) of the Tc(IV) solid phases equilibrated in $C_{\text{tot}} = 0.1$ M ($I = 5.0$ M) at $\text{pH}_m = 9.5$ (top, sample 1) and in $[\text{CO}_3^{2-}] = 1.0$ M with 0.6 M NaOH (bottom, sample 2) are shown in Fig. 7. The structural parameters obtained from the evaluation of the EXAFS data are listed in Table 2. EXAFS fits of both samples show an O-shell at 2.1 Å with a coordination number (CN) of

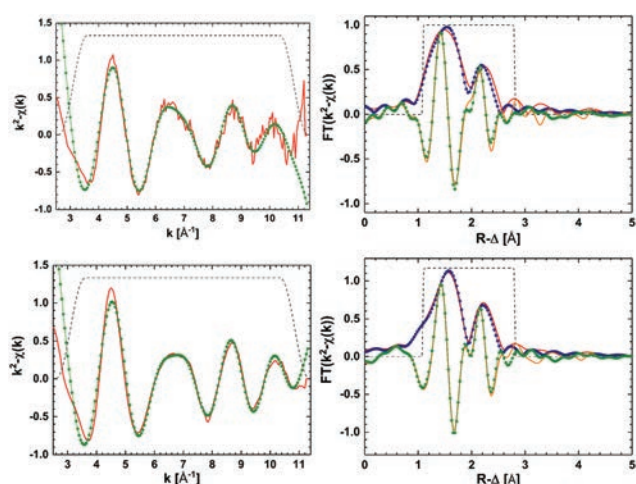


Fig. 7 k^2 Weighted EXAFS spectra and corresponding Fourier Transform of the solid phase of the sample equilibrated in $C_{\text{tot}} = 0.1$ M ($I = 5.0$ M) at $\text{pH}_m = 9.5$ (top, sample 1) and the solid phase of the sample equilibrated in $[\text{CO}_3^{2-}] = 1.0$ M with 0.6 M NaOH (bottom). Experimental data are shown as red and orange solid lines, fits are depicted as green and blue lines with circles. Dashed lines correspond to the FT hanging windows used in the EXAFS fit.

Table 2 Structural parameters obtained from the evaluation of EXAFS data for Tc(IV) solid phases equilibrated in solutions with $C_{\text{tot}} = 0.1$ M ($I = 5.0$ M) at $\text{pH}_m = 9.5$ (sample 1) and in 1.0 M $\text{Na}_2\text{CO}_3^{2-} + 0.6$ M NaOH (sample 2)

Sample	Path	CN	R [Å]	σ^2 [Å ²]	ΔE_0 [eV]	R Factor
1	Tc O	6.2	2.09	0.0087	2.1 ^a	0.018
	Tc Tc	1.3	2.58	0.0077		
2	Tc O	6.2	2.05	0.0087	2.1 ^a	0.013
	Tc Tc	1.3	2.59	0.0045		

^a ΔE_0 of both samples were defined as identical during calculations. SO^2 is fixed to 0.9. Fit errors: CN: $\pm 20\%$, R : 0.01 Å, σ^2 : ± 10 .

6.2 and a Tc-shell at 2.6 Å with a CN of 1.3. These values are in very good agreement with literature data for $\text{TcO}_2 \cdot x\text{H}_2\text{O}(\text{am})$ ^{9,54} and confirm that no solid phase transformation occurred during the course of the experiments (equilibration time ≤ 636 days). In addition, neither Cl^- nor CO_3^{2-} can be evidenced in the coordination sphere of Tc by the EXAFS fits. These results further confirm $\text{TcO}_2 \cdot 0.6\text{H}_2\text{O}(\text{am})$ as the solubility-controlling solid phase in weakly alkaline to hyperalkaline carbonate solutions.

3.5 Theoretical results

RASSCF calculations conducted for the species $\text{Tc}(\text{OH})_{m+2}\text{CO}_3^{m-}$ show that the 4s and 4p orbitals of Tc and almost all 2p orbitals of oxygen should be kept inactive. Only the two 2p orbitals of the oxygen of CO_3^{2-} in the CO_3^{2-} plane and closest to the Tc should be active. However, a comparison of CASSCF geometry optimizations with only 4d orbitals of Tc active and CASSCF calculations with a larger active space including these two 2p orbitals of O showed that their influence is negligible since their occupation number is very close to two and they can therefore safely be kept inactive, which in turn reduces the computational effort. On the basis of these results, the final active space was formed by the five 4d orbitals of Tc, which in the case of Tc(IV) are occupied with 3 electrons.

In combination with our previous work,¹⁶ these calculations show that for both systems under evaluation ($\text{TcO}(\text{OH})_m\text{CO}_3^{m-}$ and $\text{Tc}(\text{OH})_{m+2}\text{CO}_3^{m-}$), the lowest lying states are doublet and quartet states with a very clear single reference character. One of the two quartet states is lowest in energy and hence represents the ground state. This allows calculating the reaction energies of eqn (1) with DFT. This is very important, since electronic energies are much more sensitive to calculate compared to the equilibrium structures of the system and larger errors would be introduced if neglecting a multi reference character.

The structures of the species $\text{TcO}(\text{OH})_m\text{CO}_3^{m-}$ and $\text{Tc}(\text{OH})_{m+2}\text{CO}_3^{m-}$ (with $m = 1, 2$) were optimized accordingly and the total electronic energies were calculated with DFT(BP86)/TZVPP, DFT(BP86) + COSMO/TZVPP, MP2/TZVPP, CASSCF and CASPT2. These calculations were done for the naked systems in the gas phase, including solvent effects with COSMO and explicitly considering the surrounding solvent by embedding the species in a large water cluster consisting of 100 water molecules. A summary of the calculated energies for all investigated systems is provided in Table 3.

The values of ΔE summarized in Table 3 are negative and very significant for all model systems and methods used. These results clearly show that the species $\text{Tc}(\text{OH})_{m+2}\text{CO}_3^{m-}$ ($m = 1, 2$) are more stable than the corresponding dehydrated complexes $\text{TcO}(\text{OH})_m\text{CO}_3^{m-}$ ($m = 1, 2$). Note further that all applied first principle and *ab initio* methods using different model systems yield very similar structural results, which underline the validity of our theoretical calculations. The optimized structures for the naked complexes $\text{TcO}(\text{OH})_m\text{CO}_3^{m-}$ and $\text{Tc}(\text{OH})_{m+2}\text{CO}_3^{m-}$ (with $m = 1, 2$) are provided in the ESI Figure SI 1,[†] whereas the structure of the complex

Table 3 Reaction energies calculated with DFT(BP86)/TZVPP, DFT(BP86) + COSMO/TZVPP, MP2/TZVPP, CASSCF and CASPT2. Electronic energies are given in kJ mol⁻¹

$\text{TcO}(\text{OH})\text{CO}_3^- + \text{H}_2\text{O} \rightleftharpoons \text{Tc}(\text{OH})_3\text{CO}_3^-$	
DFT	74.4
COSMO	51.2
MP2	141.4
CASSCF	138.1
CASPT2	36.5
$\text{TcO}(\text{OH})_2\text{CO}_3^{2-} + \text{H}_2\text{O} \rightleftharpoons \text{Tc}(\text{OH})_4\text{CO}_3^{2-}$	
DFT	126.25
COSMO	93.54
MP2	208.3
$\text{TcO}(\text{OH})_2\text{CO}_3^{2-} + 101\text{H}_2\text{O} \rightleftharpoons \text{Tc}(\text{OH})_4\text{CO}_3^{2-} + 100\text{H}_2\text{O}$	
DFT	71.54

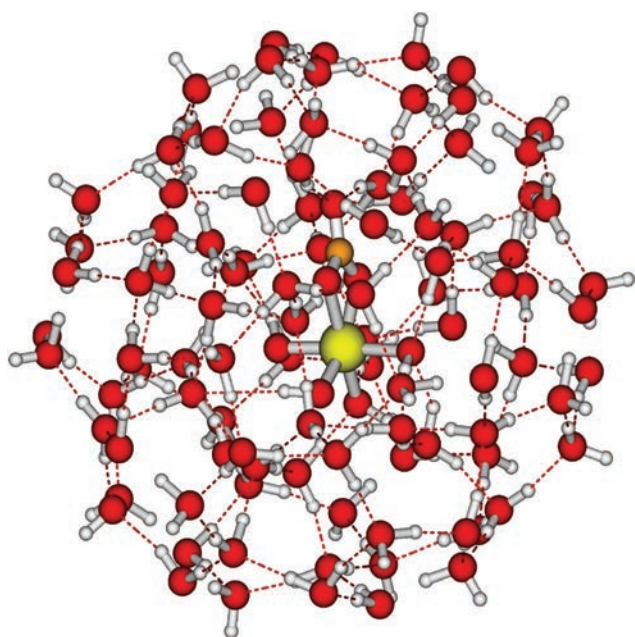


Fig. 8 Optimized structure of the complex $\text{Tc}(\text{OH})_4\text{CO}_3^{2-}$ embedded in a 100 water molecules cluster.

$\text{Tc}(\text{OH})_3\text{CO}_3^-$ embedded in a 100 water molecules cluster is shown in Fig. 8. Bond lengths of the optimized structures are also summarized in Tables SI 2 to SI 5 in the ESI.†

3.6 Chemical, thermodynamic and activity models

The chemical model describing the solution chemistry of Tc(IV) in NaHCO_3 – Na_2CO_3 – NaCl systems is derived from slope analysis of the experimental solubility data, detailed solid phase characterization and identification of solubility-controlling compounds, spectroscopic data obtained by XANES measurements and inputs on the structure of the Tc(IV)–OH– CO_3 complexes forming, provided by DFT calculations. Building on the selected chemical model, the conditional solubility constants \log^*K' are determined for each carbonate system accounting for C_{tot} and ionic strength, and then

extrapolated to $I = 0$ using the specific ion interaction theory (SIT).¹³ This approach also allows determining the SIT ion interaction coefficients of the ionic species involved in the solubility equilibria.

The SIT approach is based on extended Debye–Hückel equations in the form of a specific ion interaction term. This additional term accounts for short range, non-electrostatic interactions that have to be taken into account at concentrations of background electrolyte above ≈ 0.1 M. This approach is systematically used in the NEA-TDB. The activity coefficient of an ion j is defined by SIT as:

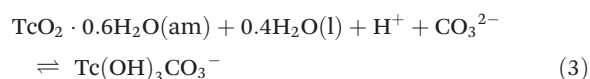
$$\log \gamma_j = z_j^2 D + \sum_k \varepsilon(j, k) m_k \quad (2)$$

where z_j is the charge of the ion j , D is the Debye–Hückel term $\left(D = \frac{A\sqrt{I_m}}{1 + Ba_j\sqrt{I_m}} \right)$, $\varepsilon(j, k)$ is the specific ion interaction coefficient of the ion j with the counter-ion k of the background electrolyte and m_k is the molality of the ion k .

Thermodynamic modelling described in this section was performed using a self-programmed Microsoft Excel® file and counterchecked using PHREEQC Interactive.⁵⁵

3.6.1 Near-neutral to alkaline conditions ($\text{pH}_m < 10.5$). Considering $\text{TcO}_2 \cdot 0.6\text{H}_2\text{O}(\text{am})$ as the solid phase controlling the solubility, the slope analysis summarized in section 3.1.1 ($\log[\text{Tc}]$ vs. pH_m and $\log[\text{Tc}]$ vs. $\log C_{\text{tot}}$) is consistent with the predominance of the complex $\text{Tc}(\text{OH})_3\text{CO}_3^-$ (or alternatively formulated as $\text{TcO}(\text{OH})\text{CO}_3^-$) in regions I and II of the solubility curves of Tc(IV) in the presence of carbonate. The formulation $\text{Tc}(\text{OH})_3\text{CO}_3^-$ is adopted in this section based on the inputs from DFT calculations performed in the present work. Note further that solubility data alone can be equally well described by Tc(IV) monomeric and polyatomic species with the same ratio $(\text{O}^{2-} + \text{OH}^-) : \text{CO}_3^{2-}$. In the absence of independent spectroscopic evidence, the monomeric notation has been favoured in this work consistent with the current NEA-TDB thermodynamic selection.

Reaction (3) is thus responsible for the control of Tc(IV) solubility at $\text{pH}_m < 10.5$, which can be accordingly expressed with chemical eqn (4) and (5) for a given background electrolyte concentration and $I = 0$, respectively.



with

$$\log^* K'_{\text{s}, \text{Tc}(\text{OH})_3\text{CO}_3} = \log[\text{Tc}(\text{OH})_3\text{CO}_3^-] - \log[\text{CO}_3^{2-}] - \log[\text{H}^+] \quad (4)$$

$$\log^* K_{\text{s}, \text{Tc}(\text{OH})_3\text{CO}_3}^{\circ} = \log^* K'_{\text{s}, \text{Tc}(\text{OH})_3\text{CO}_3} + \log \gamma_{\text{Tc}(\text{OH})_3\text{CO}_3} - \log \gamma_{\text{CO}_3^{2-}} - \log \gamma_{\text{H}^+} - 0.4 \log a_{\text{H}_2\text{O}} \quad (5)$$

The activity coefficients in eqn (5) can be calculated using the SIT formulism as shown in eqn (6). The SIT-plot resulting from the linearization of eqn (6) (*i.e.*

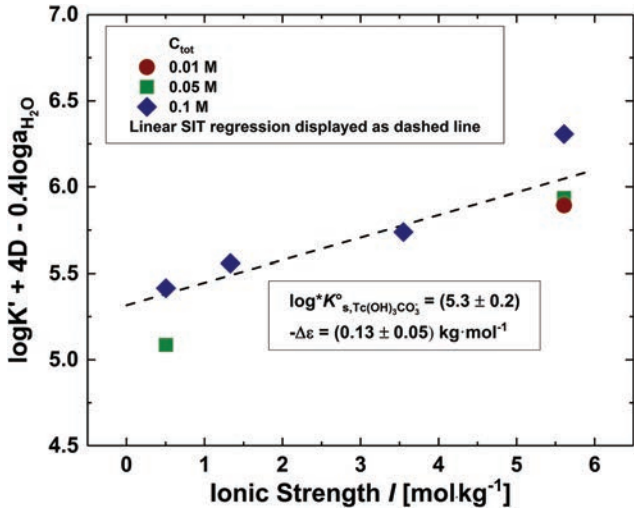
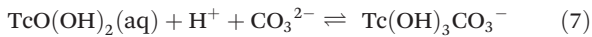


Fig. 9 SIT plot for the solubility reaction $\text{TcO}_2 \cdot 0.6\text{H}_2\text{O}(\text{am}) + 0.4\text{H}_2\text{O}(\text{l}) + \text{H}^+ + \text{CO}_3^{2-} \rightleftharpoons \text{Tc}(\text{OH})_3\text{CO}_3$ considering the conditional equilibrium constants $\log *K'_{s,\text{Tc}(\text{OH})_3\text{CO}_3}$ determined in the present work for NaHCO_3 – Na_2CO_3 – NaCl solutions with $\text{pH}_m < 10.5$.

($\log *K'_{s,\text{Tc}(\text{OH})_3\text{CO}_3} + 4D - 0.4\log a_{\text{H}_2\text{O}}$) vs. I_m) is shown in Fig. 9. Note that solubility data obtained for the system with $C_{\text{tot}} = 0.5 \text{ M}$ at $I = 5.0 \text{ M}$ (NaHCO_3 – Na_2CO_3 – NaCl) was not considered in this thermodynamic evaluation because of the significant fraction of NaCl substituted by NaHCO_3 – Na_2CO_3 (10 to 30%, depending upon pH_m).

$$\log *K'_{s,\text{Tc}(\text{OH})_3\text{CO}_3} = \log *K'_{s,\text{Tc}(\text{OH})_3\text{CO}_3} + 4D + [\varepsilon(\text{Tc}(\text{OH})_3\text{CO}_3^-, \text{Na}^+) - \varepsilon(\text{Na}^+, \text{CO}_3^{2-})] \cdot m_{\text{NaCl}} - 0.4\log a_{\text{H}_2\text{O}} \quad (6)$$

The intercept in the SIT-plot regression represents the $\log *K^\circ$ value and equals $\log *K'_{s,\text{Tc}(\text{OH})_3\text{CO}_3} = (5.3 \pm 0.2)$. The slope of the linear SIT regression corresponds to $-\Delta\varepsilon = -\varepsilon(\text{Tc}(\text{OH})_3\text{CO}_3^-, \text{Na}^+) + \varepsilon(\text{Na}^+, \text{CO}_3^{2-}) + \varepsilon(\text{H}^+, \text{Cl}^-)$, leading to $\varepsilon(\text{Tc}(\text{OH})_3\text{CO}_3^-, \text{Na}^+) = -(0.09 \pm 0.05) \text{ kg mol}^{-1}$ considering $\varepsilon(\text{Na}^+, \text{CO}_3^{2-}) = -(0.08 \pm 0.01) \text{ kg mol}^{-1}$ and $\varepsilon(\text{H}^+, \text{Cl}^-) = (0.12 \pm 0.01) \text{ kg mol}^{-1}$ as reported in Guillaumont *et al.* (2003).¹³ Combining $\log *K'_{s,\text{Tc}(\text{OH})_3\text{CO}_3}$ determined in this study with $\log *K'_{s,\text{TcO}(\text{OH})_2(\text{aq})} = (8.8 \pm 0.5)$ reported in Yalcintas *et al.* (2016) for the same $\text{TcO}_2 \cdot 0.6\text{H}_2\text{O}(\text{am})$ solid phase as used in this work, we obtain $\log *K^\circ_{\text{Tc}(\text{OH})_3\text{CO}_3} = (14.1 \pm 0.7)$ for reaction (7):



The value of $\log *K^\circ_{\text{Tc}(\text{OH})_3\text{CO}_3}$ determined in the present work is in strong disagreement with $\log *K^\circ_{\text{Tc}(\text{OH})_3\text{CO}_3} = (11.0 \pm 0.6)$ selected in the NEA-TDB.¹³ Although the formation of the $\text{Tc}(\text{OH})_3\text{CO}_3^-$ species agrees well with the slope analysis of our experimental observations, the previously reported thermodynamic and activity models for the $\text{Tc}(\text{IV})$ carbonate species cannot explain the high concentrations of $\text{Tc}(\text{IV})$ observed in our solubility study. Note that

the value of $\log *K^\circ_{\text{Tc}(\text{OH})_3\text{CO}_3}$ (or conversely $\log *K^\circ_{s,\text{Tc}(\text{OH})_3\text{CO}_3}$) originally determined by Eriksen and co-workers and later selected by the NEA-TDB was only based on a single experimental point at $\text{pH} \approx 8$ and $p_{\text{CO}_2} = 1 \text{ bar}$. As indicated by Rard and co-workers, the selection of the NEA-TDB based upon experimental solubility data reported in Eriksen *et al.* was done under the premises that “[...] their constants are selected here with increased uncertainties due to the fact that only few experimental points and no independent measurements are available”.¹² In view of the very slow kinetics observed in our solubility study, we consider it to be likely that the solubility data reported by Eriksen and co-workers may have been affected by insufficient equilibration time (supposedly a few days to few weeks). We note that $[\text{Tc}]$ measured in our solubility study in weakly alkaline carbonate systems after 15 days of equilibration time are in line with the solubility calculated using $\log *K^\circ_{\text{Tc}(\text{OH})_3\text{CO}_3}$ reported by Eriksen *et al.* and later selected by the NEA-TDB.

In order to gain further insight into the strength of the $\text{Tc}(\text{IV})$ –carbonate complexes, we have looked to other $\text{M}(\text{IV})$ – CO_3 systems of relevance in the context of nuclear waste disposal, *e.g.* $\text{Th}(\text{IV})$, $\text{Zr}(\text{IV})$ and $\text{Hf}(\text{IV})$. Comprehensive solubility experiments performed with $\text{ThO}_2(\text{am,hyd})$,⁴² $\text{ZrO}_2(\text{am})$ ⁵⁶ and $\text{HfO}_2(\text{am})$ ⁵⁷ show a very strong impact of carbonate on the solubility of these $\text{M}(\text{IV})$, in line with the strong impact observed in our solubility study with $\text{Tc}(\text{IV})$ and in contrast with the calculated solubility using the NEA-TDB thermodynamic selection for $\text{Tc}(\text{IV})$. Although all available studies describe the formation of ternary $\text{M}(\text{IV})$ – OH – CO_3 complexes in alkaline to hyperalkaline pH conditions, the stoichiometry of these complexes vary as a function of the size of the M^{4+} cation (affecting the maximum coordination number of the cation, CN). Hence, $\text{ThOH}(\text{CO}_3)_4^{5-}$ and $\text{Th}(\text{OH})_2(\text{CO}_3)_2^{2-}$ prevail for $\text{Th}(\text{IV})$ (with $r_{\text{Th}^{4+}} = 1.08 \text{ \AA}$, CN = 9)⁴⁴ whereas $\text{Zr}(\text{OH})_2(\text{CO}_3)_2^{2-}$ and $\text{Hf}(\text{OH})_2(\text{CO}_3)_2^{2-}$ were described as main ternary hydroxo-carbonate complexes for $\text{Zr}(\text{IV})$ (with $r_{\text{Zr}^{4+}} = 0.84 \text{ \AA}$, CN = 8)⁴³ and $\text{Hf}(\text{IV})$ (with $r_{\text{Hf}^{4+}} = 0.83 \text{ \AA}$, CN = 8)⁴³ respectively. The predominant role of the ternary complex $\text{Tc}(\text{OH})_3\text{CO}_3^-$ is accordingly in line with the smaller size of $\text{Tc}(\text{IV})$ (with $r_{\text{Tc}^{4+}} = 0.645 \text{ \AA}$, CN = 6).⁴³ The discussion above underpins the strong interaction of these $\text{M}(\text{IV})$ with OH^- and CO_3^{2-} , which results in strong hydrolysis and formation of sparingly soluble oxo-hydroxide solid phases, but also leads to the formation of very stable $\text{M}(\text{IV})$ – OH – CO_3 complexes.

A comparison of experimental data with solubility calculated using thermodynamic and activity models derived in this work is provided in Fig. 10a, b and c. Solubility data measured above $\text{pH}_m \approx 11$ show a tendency to increase with pH_m (see Fig. 10b and c), and thus are not properly explained with chemical and thermodynamic models assuming only the formation of the complex $\text{Tc}(\text{OH})_3\text{CO}_3^-$. As discussed in section 3.1.1, new $\text{Tc}(\text{IV})$ – OH – CO_3 complexes with a $\text{Tc}(\text{IV})$: $\text{OH} \geq 1:4$ are likely forming in this pH_m -region. These observations are further confirmed in solubility experiments conducted in Na_2CO_3 – NaOH solutions with $[\text{OH}^-] \geq 0.01 \text{ M}$, and are extensively discussed in the following section.

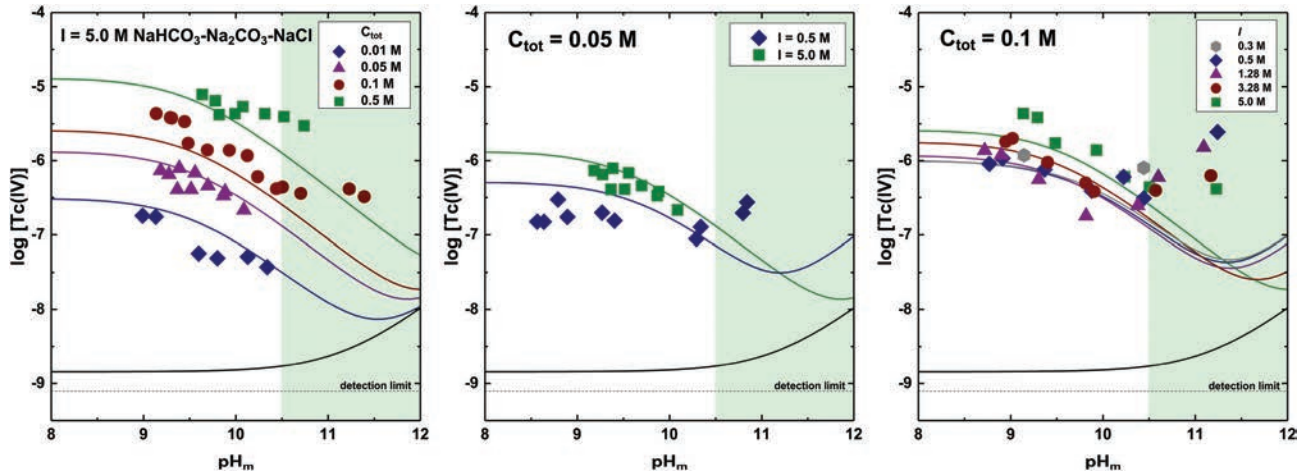
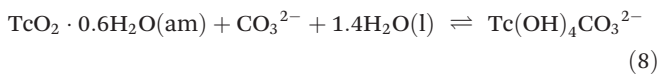


Fig. 10 Experimental solubility data of Tc(IV) in NaHCO_3 - Na_2CO_3 - NaCl systems with $8.5 \leq \text{pH}_m \leq 11.5$. Solid lines correspond to Tc(IV) solubility in the presence of carbonate calculated using thermodynamic and SIT activity models derived in the present work. Black solid line provides the reference Tc(IV) solubility in 5.0 M NaCl and absence of carbonate, as calculated with thermodynamic and SIT activity models reported in Yalcintas *et al.* (2016).⁹

3.6.2 Hyperalkaline systems ($[\text{OH}^-] \geq 0.01 \text{ M}$). There are no experimental studies available investigating the solubility of Tc(IV) in hyperalkaline carbonate-containing solutions. The two chemical species reported in the literature (Tc(OH)₂CO₃(aq) and Tc(OH)₃CO₃⁻, the latter confirmed also in the present study) do not form in hyperalkaline conditions ($\text{pH}_m > 11$) where the hydrolysis species TcO(OH)₃⁻ was accordingly expected to prevail. However, our solubility data at $10.5 \leq \text{pH}_m \leq 11.5$ (NaHCO_3 - Na_2CO_3 - NaCl systems) and $[\text{OH}^-] \geq 0.01 \text{ M}$ (Na_2CO_3 - NaOH systems) suggest the formation of previously unreported Tc(IV)-OH-CO₃ complex(es). Slope analysis summarized in section 3.1.2 indicates that a pH_m -independent equilibrium reaction controls the solubility of Tc(IV) in the more concentrated carbonate systems. This observation combined with a solubility-control by TcO₂·0.6H₂O(am) as confirmed by solid phase characterization in section 3.3 is consistent with the predominance of the complex Tc(OH)₄CO₃²⁻ in the aqueous phase. Note that the formation of the complex Tc(OH)₄(CO₃)₂⁴⁻ is consistent also with a slope of ≈ 0 in the solubility diagram, but such a species is considered unlikely in view of the small size of Tc⁴⁺ (ionic radii = 0.645 Å) and the restricted coordination number around the metal cation (CN = 6).^{4,3} Reaction (8) can accordingly be defined



with

$$\log *K'_{\text{s,Tc}(\text{OH})_4\text{CO}_3^{2-}} = \log[\text{Tc}(\text{OH})_4\text{CO}_3^{2-}] - \log[\text{CO}_3^{2-}] \quad (9)$$

$$\log *K_{\text{s,Tc}(\text{OH})_4\text{CO}_3^{2-}}^{\circ} = \log *K'_{\text{s,Tc}(\text{OH})_4\text{CO}_3^{2-}} + \log \gamma_{\text{Tc}(\text{OH})_4\text{CO}_3^{2-}} \\ \log \gamma_{\text{CO}_3^{2-}} \quad 1.4 \log a_{\text{H}_2\text{O}} \quad (10)$$

Activity coefficients in eqn (10) are calculated using the SIT approach. The SIT-plot resulting from eqn (11) is shown in Fig. 11.

$$\log *K_{\text{s,Tc}(\text{OH})_4\text{CO}_3^{2-}}^{\circ} = \log *K'_{\text{s,Tc}(\text{OH})_4\text{CO}_3^{2-}} + [\varepsilon(\text{Tc}(\text{OH})_4\text{CO}_3^{2-}, \text{Na}^+) \\ \varepsilon(\text{Na}^+, \text{CO}_3^{2-})] \cdot m_{\text{NaCl}} - 1.4 \log a_{\text{H}_2\text{O}} \quad (11)$$

Linear regression in Fig. 11 was conducted using only $\log *K'_{\text{s,Tc}(\text{OH})_4\text{CO}_3^{2-}}$ values derived from solubility data following a slope of ≈ 0 in 0.5 and 1.0 M Na₂CO₃ systems (full symbols in Fig. 11) (see section 3.1.2 and discussion above). It

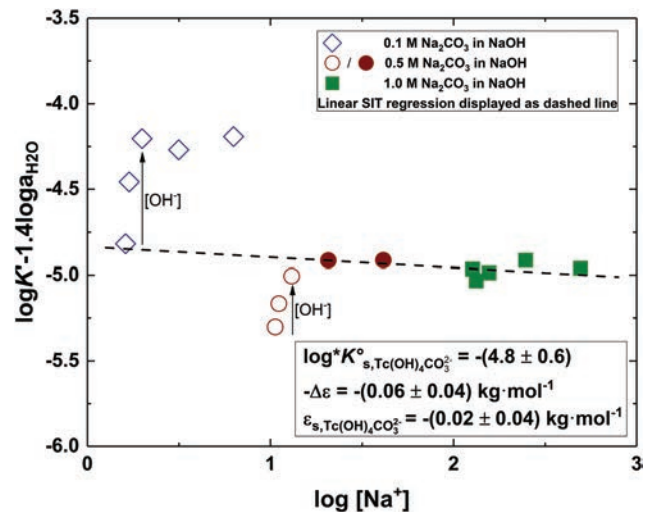


Fig. 11 SIT plot for the solubility reaction $\text{TcO}_2 \cdot 0.6\text{H}_2\text{O}(\text{am}) + \text{CO}_3^{2-} + 1.4\text{H}_2\text{O}(\text{l}) \rightleftharpoons \text{Tc}(\text{OH})_4\text{CO}_3^{2-}$ considering the conditional $\log *K'_{\text{s,Tc}(\text{OH})_4\text{CO}_3^{2-}}$ determined in the present work for carbonate solutions. Linear regression performed considering only full symbols (see text for explanations).

is clear that $\log *K'_{s, \text{Tc}(\text{OH})_4\text{CO}_3^{2-}}$ values represented by empty points do not follow the linear trend of the SIT-plot, and thus likely relate to a different chemical reaction. For these experimental data, the increased stability with increasing $[\text{Na}^+]$ (which correlates with increasing $[\text{OH}^-]$) may hint towards an increased number of OH-groups in the first coordination shell of Tc(IV). However, attempts to model these data by including *e.g.* the complexes $\text{Tc}(\text{OH})_5\text{CO}_3^{3-}$ or $\text{Tc}(\text{OH})_5(\text{CO}_3)_2^{5-}$ were not successful.

Several difficulties prevent the definition of a definitive chemical model for the system Tc(IV)–carbonate under hyperalkaline conditions:

- Solubility data at lower carbonate concentrations are not properly explained considering only the formation of the complex $\text{Tc}(\text{OH})_4\text{CO}_3^{2-}$ (or analogous polynuclear species). The definition of additional complexes with increased Tc : OH ratios (*e.g.* $\text{Tc}(\text{OH})_5\text{CO}_3^{3-}$ or $\text{Tc}(\text{OH})_5(\text{CO}_3)_2^{5-}$) does not improve the quality of the fit either.

- The time dependency of the solubility shown in Fig. 4a suggests that equilibrium conditions may have not been attained in 0.1 M Na_2CO_3 systems with $0.01 \text{ M} \leq [\text{OH}^-] \leq 0.6 \text{ M}$, even after an equilibration time of ≈ 450 days.

- Experimental observations at high carbonate concentrations ($[\text{CO}_3^{2-}] \geq 0.5 \text{ M}$) can be properly explained by claiming the formation of the complex $\text{Tc}(\text{OH})_4\text{CO}_3^{2-}$. A simplified model involving the equilibrium of this monomeric species with $\text{TcO}_2 \cdot 0.6\text{H}_2\text{O}(\text{am})$ is however challenged by the very long equilibration kinetics observed (up to 400 days in some cases). As described for Tc(IV) acidic solutions in the absence of carbonate, such behaviour may indicate the formation of polyatomic species. Note that solubility data for these carbonate concentrations can be equally well described by polyatomic species with the same ratio ($\text{O}^{2-} + \text{OH}^-$) : CO_3^{2-} (*e.g.* $\text{Tc}_2\text{O}_2(\text{OH})_4(\text{CO}_3)_2^{4-}$, $\text{Tc}_3\text{O}_4(\text{OH})_4(\text{CO}_3)_3^{6-}$, *etc.*).

For the reasons summarized above, the stoichiometry of the complex $\text{Tc}(\text{OH})_4\text{CO}_3^{2-}$ proposed to form in hyperalkaline conditions is considered only as tentative. Although possibly correct, this chemical model is considered incomplete and likely requires the definition of additional Tc(IV)–OH– CO_3 complexes which at present remain undefined. Further experimental efforts are on-going at KIT–INE to close this gap in the aqueous chemistry of Tc(IV) in hyperalkaline carbonate solutions.

3.6.3 Chemical, thermodynamic and activity models for the system $\text{Tc}^{4+}\text{-Na}^+\text{-H}^+\text{-Cl}^-\text{-OH}^-\text{-HCO}_3^-\text{-CO}_3^{2-}\text{-H}_2\text{O}(\text{l})$.

Table 4 summarizes thermodynamic data derived in the present work for Tc(IV) in $\text{NaHCO}_3\text{-Na}_2\text{CO}_3\text{-NaCl}$ systems, as well as data previously obtained within our research group for Tc(IV) in carbonate-free NaCl systems. Table 4 includes also the equilibrium constant selected in the NEA–TDB for the complex $\text{Tc}(\text{OH})_2\text{CO}_3(\text{aq})$, which becomes predominant in weakly acidic to near-neutral carbonate solutions. Although our experimental solubility data does not cover this pH-range, discrepancies observed with the reported stability of $\text{Tc}(\text{OH})_3\text{CO}_3^-$ suggest that $\log *K'_{s, \text{Tc}(\text{OH})_2\text{CO}_3}$ might be largely underestimated. Table 5 provides SIT ion interaction coefficients of all Tc(IV) aqueous species described in Table 4. In spite of the experimental evidence on the formation of additional Tc(IV)–OH– CO_3 complexes in hyperalkaline conditions, our solubility data does not provide a conclusive proof of the stoichiometry of these species and thus the validity of the reported models is limited to $\text{pH}_m < 11$.

The predominance diagrams in Fig. 12 and 13 show the impact of carbonate on the aqueous speciation of Tc(IV) calculated for $C_{\text{tot}} = 2 \times 10^{-3} \text{ M}$ (0.1 M NaCl systems) and $C_{\text{tot}} = 0.1 \text{ M}$ (5.0 M NaCl systems), respectively, using the thermodynamic data and SIT coefficients summarized in Tables 4 and 5. Calculations were performed using Spana – Chemical Equilibrium Diagrams software.^{58–60} The dark green field in both diagrams corresponds to the formation of the complex “ $\text{Tc}(\text{OH})_4\text{CO}_3^{2-}$ ”. Although the stoichiometry of this species has not been unequivocally established yet, the dark green field provides a qualitative insight on the expected formation of carbonate complexes of Tc(IV) in hyperalkaline pH_m -conditions, which so far was not investigated in previous experimental studies.

Fig. 12 shows that carbonate has a significant impact on the aqueous speciation of Tc(IV) at the low C_{tot} expected in granitic groundwaters ($C_{\text{tot}} = 2 \times 10^{-3} \text{ M}$ in Fig. 12).^{61–63} At this C_{tot} , the complex $\text{Tc}(\text{OH})_3\text{CO}_3^-$ becomes predominant within $\text{pH}_m \approx 5\text{-}10.5$, whereas the formation of ternary complexes with higher Tc : OH ratio (“ $\text{Tc}(\text{OH})_4\text{CO}_3^{2-}$ ”, dark green field in Fig. 12) takes place only within a narrower pH_m -range, $\approx 10\text{-}11.5$. In spite of the predominant role of the Tc(IV)–OH– CO_3 complexes, the redox borderline $\text{Tc}(\text{VII})_{\text{aq}}/\text{Tc}(\text{IV})_{\text{aq}}$ in the presence of carbonate remains almost unaffected compared to

Table 4 Equilibrium reactions and corresponding stability constants derived in this work and reported in Yalcintas *et al.* (2016) and NEA TDB for the system $\text{Tc}^{4+}\text{-Na}^+\text{-H}^+\text{-Cl}^-\text{-OH}^-\text{-HCO}_3^-\text{-CO}_3^{2-}\text{-H}_2\text{O}(\text{l})$ ^{9,13}

Reactions	SIT $\log *K^\circ$	Ref.
$\text{TcO}_2 \cdot 0.6\text{H}_2\text{O}(\text{am}) + \frac{2}{3}\text{H}^+ \rightleftharpoons \frac{1}{3}\text{Tc}_3\text{O}_5^{2+} + \frac{2.8}{3}\text{H}_2\text{O}(\text{l})$	(1.5 ± 0.2)	9
$\text{TcO}_2 \cdot 0.6\text{H}_2\text{O}(\text{am}) + 0.4\text{H}_2\text{O}(\text{l}) \rightleftharpoons \text{TcO}(\text{OH})_2(\text{aq})$	(8.8 ± 0.5)	9
$\text{TcO}_2 \cdot 0.6\text{H}_2\text{O}(\text{am}) + 1.4\text{H}_2\text{O}(\text{l}) \rightleftharpoons \text{TcO}(\text{OH})_3^- + \text{H}^+$	$(19.27 \pm 0.06) / (19.0 \pm 0.2)$	9/48
$\text{TcO}_2 \cdot 0.6\text{H}_2\text{O}(\text{am}) + 2\text{H}^+ + \text{CO}_3^{2-} \rightleftharpoons \text{Tc}(\text{OH})_2\text{CO}_3(\text{aq}) + 0.6\text{H}_2\text{O}(\text{l})$	$(10.5 \pm 2.0)^a$	13
$\text{TcO}_2 \cdot 0.6\text{H}_2\text{O}(\text{am}) + 0.4\text{H}_2\text{O}(\text{l}) + \text{H}^+ + \text{CO}_3^{2-} \rightleftharpoons \text{Tc}(\text{OH})_3\text{CO}_3^-$	(5.3 ± 0.2)	p.w.

^a Uncertainty increased in this work to account for the likely underestimation of the $\log *K^\circ$ value.

Table 5 SIT ion interaction coefficients for Tc(IV) hydrolysis species and carbonate complexes as determined in this work or reported in Yalcintas *et al.* (2016)

i	j	SIT $\epsilon(i,j)$	Ref.
Tc ₃ O ₅ ²⁺	Cl ⁻	(0.41 ± 0.05)	9
Na ⁺	TcO(OH) ₃ ⁻	(0.09 ± 0.02)	9
Na ⁺	Tc(OH) ₂ CO ₃ (aq)	0	^a
Na ⁺	Tc(OH) ₃ CO ₃ ⁻	(0.09 ± 0.05)	p.w.

^a By definition in SIT.

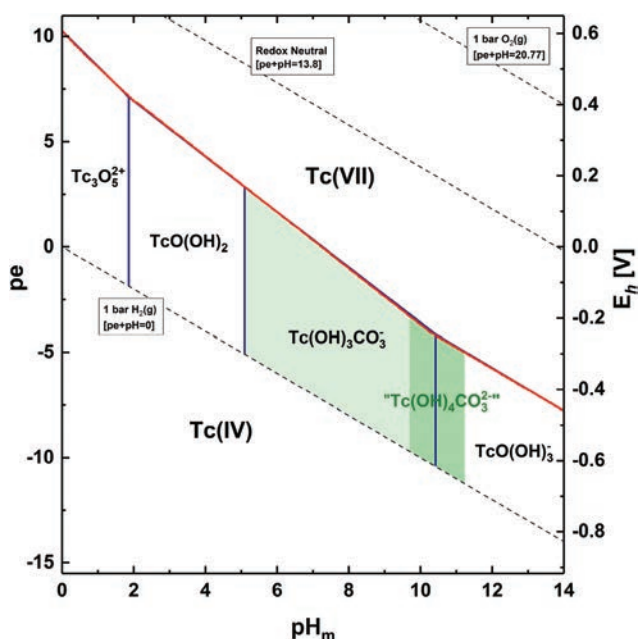


Fig. 12 Predominance diagrams of Tc calculated for $C_{\text{tot}} = 2 \times 10^{-3}$ M, 0.1 M NaCl; using the thermodynamic data and SIT coefficients summarized in Tables 4 and 5. Calculations performed for $[\text{Tc}]_{\text{tot}} = 10^{-9}$ M. Red line corresponds to the redox borderline $\text{Tc(VII)}_{\text{aq}}/\text{Tc(IV)}_{\text{aq}}$ calculated for the same boundary conditions but in the absence of carbonate.

carbonate-free systems (red line in Fig. 12). At higher carbonate concentrations (Fig. 13, $C_{\text{tot}} = 0.1$ M, 5.0 M NaCl), ternary $\text{Tc(IV)}\text{-OH-CO}_3$ complexes control the aqueous speciation of Tc(IV) within $\text{pH}_m \approx 3.5\text{-}11.5$. This elevated carbonate concentration affects also the redox borderline $\text{Tc(VII)}_{\text{aq}}/\text{Tc(IV)}_{\text{aq}}$, which is displaced almost one pe-unit towards more oxidizing conditions (see red line in Fig. 13).

As observed in our experimental results, the great impact of carbonate on the aqueous speciation of Tc(IV) strongly affects solubility but, similarly, may affect sorption processes under conditions relevant for nuclear waste disposal.⁶⁴

4 Conclusions

The solubility of Tc(IV) was systematically investigated as a function of carbonate concentration, ionic strength and pH_m /

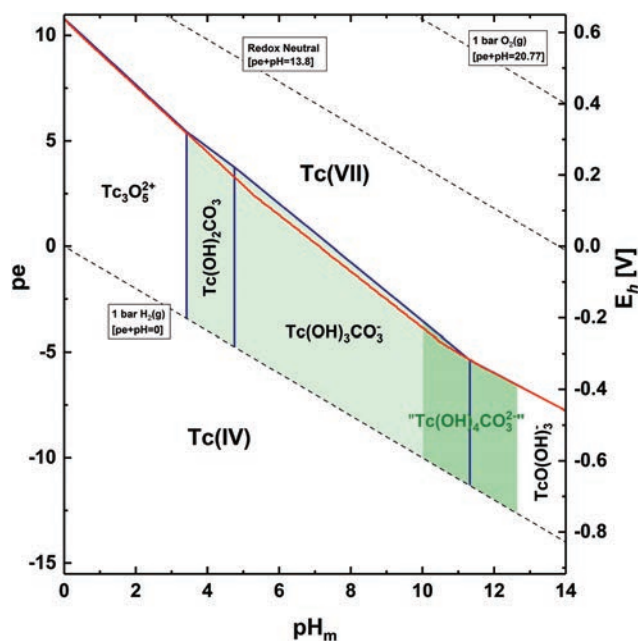


Fig. 13 Predominance diagrams of Tc calculated for $C_{\text{tot}} = 0.1$ M, 5.0 M NaCl using the thermodynamic data and SIT coefficients summarized in Tables 4 and 5. Calculations performed for $[\text{Tc}]_{\text{tot}} = 10^{-9}$ M. Red line corresponds to the redox borderline $\text{Tc(VII)}_{\text{aq}}/\text{Tc(IV)}_{\text{aq}}$ calculated for the same boundary conditions but in the absence of carbonate.

$[\text{OH}^-]$. Solid phase characterization by XAFS, XRD, SEM-EDS, quantitative chemical analysis and TG-DTA identified the solubility-controlling solid phase as $\text{TcO}_2 \cdot 0.6\text{H}_2\text{O(am)}$ in agreement with earlier studies in carbonate-free NaCl solutions. Redox speciation by liquid-liquid extraction and XANES confirmed the predominance of Tc(IV) aqueous species under the conditions investigated in the present work. A strong effect of carbonate was observed in all investigated samples, leading to up to 3.5 orders of magnitude greater solubility than in carbonate-free systems. Very long contact time ($t \geq 275$ days) was required to attain equilibrium conditions in most of the solubility systems investigated. This is possibly the reason for the significant discrepancies observed with previous solubility studies, where much shorter equilibration times may have led to the underestimation of the carbonate effect on the solubility of Tc(IV) .

Slope analysis of solubility data combined with solid phase characterization and DFT calculations indicate that the complex $\text{Tc(OH)}_3\text{CO}_3^-$ is predominant in carbonate solutions at $8.5 \leq \text{pH}_m \leq 11$. Although this observation is consistent with the chemical model adopted in the NEA-TDB, thermodynamic and activity models derived in this work highlight that the stability of this complex was largely underestimated in previous thermodynamic studies.

Above $\text{pH}_m \approx 11$, solubility data suggest also the formation of previously unreported $\text{Tc(IV)}\text{-OH-CO}_3$ complex(es), possibly $\text{Tc(OH)}_4\text{CO}_3^{2-}$. However, the pH_m -dependency of the solubility observed for $C_{\text{tot}} = 0.1$ M and $[\text{OH}^-] \geq 0.01$ M and the very slow kinetics (increasing $[\text{Tc}]$ with time for $t \leq 450$ days) may also

hint towards the formation/predominance of additional Tc(IV)-OH-CO₃ complexes. Our data do not yet allow to parametrize these observations in a thermodynamic model. Further investigations targeting this hyperalkaline pH_m-region are on-going at KIT-INE.

This work provides robust solubility upper limits that allow estimating the source-term of Tc(IV) in carbonate-containing alkaline systems. It further represents the most comprehensive thermodynamic dataset available to date for the system Tc⁴⁺-Na⁺-H⁺-Cl⁻-OH⁻-HCO₃⁻-CO₃²⁻-H₂O(l), which can be implemented in thermodynamic databases and geochemical calculations extending over a wide range of conditions relevant for nuclear waste disposal. Thermodynamic datagaps identified in this study can be relevant for the assessment of Tc(IV) chemistry under hyperalkaline conditions as those expected in cementitious systems and deserve further attention.

Conflicts of interest

There are no conflicts to declare.

Acknowledgements

The authors would like to thank M. Böttle, N. Finck, S. Heck, S. Moisei-Rabung, V. Montoya and D. Schild (KIT-INE) for their lab assistance and for performing XRD analyses, TG-DTA, ICP-OES and SEM-EDS measurements.

References

- 1 H. Geckeis, K.-J. Röhlig and K. Mengel, *Chem. Unserer Zeit*, 2012, **46**, 282–293.
- 2 Reaktor-Sicherheitskommission, *Gase im Endlager (Beratungsauftrag RS III 2-17015/8 vom 27.04.2004)*, Bonn, 2005.
- 3 W. Brewitz, *GSF-T 114*, Braunschweig, 1980.
- 4 S. K. Frape and P. Fritz, *Geochim. Cosmochim. Acta*, 1984, **48**, 1617–1627.
- 5 V. Neck, M. Altmaier, T. Rabung, J. Lützenkirchen and T. Fanghänel, *Pure Appl. Chem.*, 2009, **81**, 1555–1568.
- 6 D. Fellhauer, J. Rothe, M. Altmaier, V. Neck, J. Runke, T. Wiss and T. Fanghänel, *Radiochim. Acta*, 2016, **104**, 355–379.
- 7 D. Fellhauer, V. Neck, M. Altmaier, J. Lützenkirchen and T. Fanghänel, *Radiochim. Acta*, 2010, **98**, 541–548.
- 8 M. Altmaier, V. Neck and T. Fanghänel, *Radiochim. Acta*, 2008, **96**, 541–550.
- 9 E. Yalcintas, X. Gaona, M. Altmaier, K. Dardenne, R. Polly and H. Geckeis, *Dalton Trans.*, 2016, **45**, 8916–8936.
- 10 T. E. Eriksen, P. Ndalamba, J. Bruno and M. Caceci, *Radiochim. Acta*, 1992, **58/59**, 67–70.
- 11 T. E. Eriksen, P. Ndalamba, D. Cui, J. Bruno, M. Caceci and K. Spahiu, *SKB Tech. Rep.*, 1993, 93–18.
- 12 J. A. Rard, M. H. Rand, G. Anderegg and H. Wanner, *Chemical Thermodynamics of Technetium*, North Holland Elsevier Science Publishers B. V., Amsterdam, The Netherlands, 1999.
- 13 R. Guillaumont, T. Fanghänel, J. Fuger, I. Grenthe, V. Neck, D. A. Palmer and M. H. Rand, *Update on the Chemical Thermodynamics of U, Np, Pu, Am and Tc*, North Holland Elsevier Science Publishers B. V., Amsterdam, The Netherlands, 2003.
- 14 D. J. Liu, J. Yao, B. Wang, C. Bruggeman and N. Maes, *Radiochim. Acta*, 2007, **95**, 523–528.
- 15 I. Alliot, C. Alliot, P. Vitorge and M. Fattahi, *Environ. Sci. Technol.*, 2009, **43**, 9174–9182.
- 16 R. Polly, B. Schimmelpfennig, E. Yalcintas, X. Gaona and M. Altmaier, Tc(IV) hydrolysis species and ternary Na/Ca-TcIV-OH complexes in alkaline CaCl₂ and NaCl solutions: a quantum chemical study, *Migratiopn'15*, Santa Fe, New Mexico, USA, 2015.
- 17 K. G. Knauss, T. J. Wolery and K. J. Jackson, *Geochim. Cosmochim. Acta*, 1990, **54**, 1519–1523.
- 18 V. Neck, M. Altmaier, R. Müller, V. Metz and B. Kienzler, *Experimentelles Programm zur Bestätigung der Ergebnisse von standortspezifischen Modellrechnungen für die Schachanlage Asse, Teil 3: Löslichkeitsexperimente zur Absicherung der thermodynamischen Datenbasis*, Institute for Nuclear Waste Disposal (INE), Forschungszentrum Karlsruhe, 2003.
- 19 M. Altmaier, V. Metz, V. Neck, R. Müller and T. Fanghänel, *Geochim. Cosmochim. Acta, Suppl.*, 2003, **67**, 3595–3601.
- 20 M. Altmaier, F. Bok, X. Gaona, C. Marquardt, V. Montoya, H. C. Moog, A. Richter, T. Scharge, W. Voigt and S. Wilhelm, THEREDA Thermodynamische Referenz-Datenbasis, Report 978-3-944161-77-8, 2015.
- 21 H. C. Moog, F. Bok, C. M. Marquardt and V. Brendler, *Appl. Geochem.*, 2015, **55**, 72–84.
- 22 R. Kopunec, F. N. Abudeab and S. Skragkovfi, *J. Radioanal. Nucl. Chem.*, 1998, **230**, 51–60.
- 23 E. Yalcintas, X. Gaona, A. C. Scheinost, T. Kobayashi, M. Altmaier and H. Geckeis, *Radiochim. Acta*, 2015, **103**, 57–72.
- 24 T. Kobayashi, A. C. Scheinost, D. Fellhauer, X. Gaona and M. Altmaier, *Radiochim. Acta*, 2013, **101**, 323–332.
- 25 A. Zimina, K. Dardenne, M. A. Denecke, D. E. Doronkin, E. Huttel, H. Lichtenberg, S. Mangold, T. Pruessmann, J. Rothe, T. Spangenberg, R. Steininger, T. Vitova, H. Geckeis and J.-D. Grunwaldt, *Rev. Sci. Instrum.*, 2017, **88**, 113113.
- 26 Karlsruhe Institute of Technology (KIT), ANKA - Test Facility and Synchrotron Radiation Source, <http://www.anka.kit.edu>, (accessed 01.06.2017).
- 27 B. Ravel and M. Newville, *J. Synchrotron Radiat.*, 2005, **12**, 537–541.
- 28 F. Aquilante, J. Autschbach, R. K. Carlson, L. F. Chibotaru, M. G. Delcey, L. D. Vico, I. F. Galvan, N. Ferré, L. M. Frutos, L. Gagliardi, M. Garavelli, A. Giussani, C. E. Hoyer, G. L. Manni, H. Lischka, D. Ma, P. Å. Malmqvist, T. Müller, A. Nenov, M. Olivucci, T. B. Pedersen, D. Peng, F. Plasser, B. Pritchard, M. Reiher, I. Rivalta, I. Schapiro, J. Segarra-

- Marti, M. Stenrup, D. G. Truhlar, L. Ungur, A. Valentini, S. Vancoillie, V. Veryazov, V. P. Vysotskiy, O. Weingart, F. Zapata and R. Lindh, *J. Comput. Chem.*, 2016, **37**, 506–541.
- 29 B. O. Roos, R. Lindh, P.-A. Malmqvist, V. Veryazov and P.-O. Widmark, *J. Phys. Chem. A*, 2005, **109**, 6575–6579.
- 30 B. O. Roos, R. Lindh, P.-Å. Malmqvist, V. Veryazov and P.-O. Widmark, *J. Phys. Chem. A*, 2004, **108**, 2851–2858.
- 31 P.-O. Widmark, P.-A. Malmqvist and B. O. Roos, *Theor. Chim. Acta*, 1990, **77**, 291–306.
- 32 A. Schäfer, C. Huber and R. Ahlrichs, *J. Chem. Phys.*, 1994, **100**, 5829–5835.
- 33 *TURBOMOLE V7.0 2015*, University of Karlsruhe and Forschungszentrum Karlsruhe GmbH, 1989–2007.
- 34 O. Treutler and R. Ahlrichs, *J. Chem. Phys.*, 1995, **102**, 346–354.
- 35 K. Eichkorn, F. Weigend, O. Treutler and R. Ahlrichs, *Theor. Chem. Acc.*, 1997, **97**, 119–124.
- 36 K. Eichkorn, O. Treutler, H. Öhm, M. Häser and R. Ahlrichs, *Chem. Phys. Lett.*, 1995, **242**, 283–290.
- 37 P. Deglmann, K. May, F. Furche and R. Ahlrichs, *Chem. Phys. Lett.*, 2004, **384**, 103–107.
- 38 M. v. Arnim and R. Ahlrichs, *J. Chem. Phys.*, 1999, **111**, 9183–9190.
- 39 A. Schäfer, H. Horn and R. Ahlrichs, *J. Chem. Phys.*, 1992, **97**, 2571–2577.
- 40 A. Lenz and L. Ojamäe, *J. Mol. Struct.: THEOCHEM*, 2009, **944**, 163–167.
- 41 A. Lenz, *PhD Thesis*, Linköping Universitet, 2009.
- 42 M. Altmaier, V. Neck, R. Müller and T. Fanghänel, *Radiochim. Acta*, 2005, **93**, 83.
- 43 J. C. Shannon, Database of Ionic Radii, <http://abulafia.mt.ic.ac.uk/shannon/ptable.php>, (accessed 01.06.2017).
- 44 V. Neck and J. I. Kim, *Radiochim. Acta*, 2001, **89**, 1–16.
- 45 W. Ostwald, *Z. Phys. Chem.*, 1897, **22U**, 289.
- 46 F. Poineau, *PhD Thesis*, Université de Nantes, 2004.
- 47 H. Gamsjäger, T. Gajda, J. Sangster, S. K. Saxena and W. Voigt, *Chemical Thermodynamics Of Tin*, OECD Publications, Paris, France, 2012.
- 48 A. Baumann, E. Yalcintas, X. Gaona, M. Altmaier and H. Geckeis, *New J. Chem.*, 2017, **41**, 9077–9086.
- 49 P. G. Allen, G. S. Siemering, D. K. Shuh, J. J. Bucher, N. M. Edelstein, C. A. Langton, S. B. Clark, T. Reich and M. A. Denecke, *Radiochim. Acta*, 1997, **76**, 77.
- 50 S. A. Saslow, W. Um, C. I. Pearce, M. H. Engelhard, M. E. Bowden, W. Lukens, I. I. Leavy, B. J. Riley, D.-S. Kim, M. J. Schweiger and A. A. Kruger, *Environ. Sci. Technol.*, 2017, **51**, 8635–8642.
- 51 W. W. Lukens, D. K. Shuh, N. C. Schroeder and K. R. Ashley, *Environ. Sci. Technol.*, 2004, **38**, 229–233.
- 52 U. Mazzi, R. Schibli, H.-J. Pietzsch, J.-U. Künstler and H. Spies, *Technetium-99m Pharmaceuticals*, Springer, Berlin, Heidelberg, 2007.
- 53 F. Poineau, M. Fattahi, C. D. Auwer, C. Hennig and B. Grambow, *Radiochim. Acta*, 2006, **94**, 283–289.
- 54 N. J. Hess, Y. Xia, D. Rai and S. D. Conradson, *J. Solution Chem.*, 2004, **33**, 199–226.
- 55 D. L. Parkhurst and C. A. J. Appelo, PHREEQC (Version 3)–A Computer Program for Speciation, Batch-Reaction, One-Dimensional Transport, and Inverse Geochemical Calculations, https://wwwbrr.cr.usgs.gov/projects/GWC_coupled/index.html, (accessed 28.07.2017, 2017).
- 56 T. Kobayashi and T. Sasaki, *J. Solution Chem.*, 2017, **46**, 1741–1759.
- 57 D. Rai, A. Kitamura and K. M. Rosso, *Radiochim. Acta*, 2017, **105**, 637.
- 58 I. Puigdomenech, Spana, <https://sites.google.com/site/chemdiagr/>, (accessed 01.08.2017).
- 59 I. Puigdomenech, *INPUT, SED, and PREDOM: Computer programs drawing equilibrium diagrams*, Royal Institute of Technology (KTH), Dept. Inorg. Chemistry, Stockholm, Sweden, 1983.
- 60 I. Puigdomenech, presented in part at the 219th ACS National Meeting, San Francisco, March 26–30, 2000.
- 61 L. Duro, M. Grivé, E. Cera, X. Gaona, C. Domènech and J. Bruno, *TR-06-32 - Determination and assessment of the concentration limits to be used in SR-Can*, Stockholm, Sweden, 2006.
- 62 L. F. Auqué, M. J. Gimeno, J. B. Gómez, I. Puigdomenech, J. Smellie and E.-L. Tullborg, *TR-06-31 - Groundwater chemistry around a repository for spent nuclear fuel over a glacial cycle*, Stockholm, Sweden, 2006.
- 63 R. S. Forsyth, L. O. Werme and J. Bruno, *TR-85-16 - The corrosion of spent UO₂ fuel in synthetic groundwater*, Stockholm, Sweden, 1985.
- 64 F. M. Huber, Y. Totskiy, R. Marsac, D. Schild, I. Pidchenko, T. Vitova, S. Kalmykov, H. Geckeis and T. Schäfer, *Appl. Geochem.*, 2017, **80**, 90–101.

Repository KITopen

Dies ist ein Postprint/begutachtetes Manuskript.

Empfohlene Zitierung:

Baumann, A.; Yalçıntaş, E.; Gaona, X.; Polly, R.; Dardenne, K.; Prüßmann, T.; Rothe, J.; Altmaier, M.; Geckeis, H.

[Thermodynamic description of Tc\(IV\) solubility and carbonate complexation in alkaline NaHCO₃-Na₂CO₃-NaCl systems](#)

2018. Dalton transactions, 47

[doi: 10.554/IR/1000083664](#)

Zitierung der Originalveröffentlichung:

Baumann, A.; Yalçıntaş, E.; Gaona, X.; Polly, R.; Dardenne, K.; Prüßmann, T.; Rothe, J.; Altmaier, M.; Geckeis, H.

[Thermodynamic description of Tc\(IV\) solubility and carbonate complexation in alkaline NaHCO₃-Na₂CO₃-NaCl systems](#)

2018. Dalton transactions, 47 (12), 4377–4392.

[doi:10.1039/C8DT00250A](#)

Lizenzinformationen: [KITopen-Lizenz](#)